CHEMISTRY
A EUROPEAN JOURNAL

DOI: 10.1002/chem.200600564

Orbital Overlap and Chemical Bonding

Andreas Krapp,[a] F. Matthias Bickelhaupt,*[b] and Gernot Frenking*[a]

Dedicated to Professor Rolf Gleiter on the occasion of his 70th birthday

Abstract: The chemical bonds in the diatomic molecules Li_2–F_2 and Na_2–Cl_2 at different bond lengths have been analyzed by the energy decomposition analysis (EDA) method using DFT calculations at the BP86/TZ2P level. The interatomic interactions are discussed in terms of quasiclassical electrostatic interactions ΔE_{elstat}, Pauli repulsion ΔE_{Pauli} and attractive orbital interactions ΔE_{orb}. The energy terms are compared with the orbital overlaps at different interatomic distances. The quasiclassical electrostatic interactions between two electrons occupying 1s, 2s, 2p(σ), and 2p(π) orbitals have been calculated and the results are analyzed and discussed. It is shown that the equilibrium distances of the covalent bonds are not determined by the maximum overlap of the σ valence orbitals, which nearly always has its largest value at clearly shorter distances than the equilibrium bond length. The crucial interaction that prevents shorter bonds is not the loss of attractive interactions, but a sharp increase in the Pauli repulsion between electrons in valence orbitals. The attractive interactions of ΔE_{orb} and the repulsive interactions of ΔE_{Pauli} are both determined by the orbital overlap. The net effect of the two terms depends on the occupation of the valence orbitals, but the onset of attractive orbital interactions occurs at longer distances than Pauli repulsion, because overlap of occupied orbitals with vacant orbitals starts earlier than overlap between occupied orbitals. The contribution of ΔE_{elstat} in most nonpolar covalent bonds is strongly attractive. This comes from the deviation of quasiclassical electron–electron repulsion and nuclear–electron attraction from Coulomb's law for point charges. The actual strength of ΔE_{elstat} depends on the size and shape of the occupied valence orbitals. The attractive electrostatic contributions in the diatomic molecules Li_2–F_2 come from the s and p(σ) electrons, while the p(π) electrons do not compensate for nuclear–nuclear repulsion. It is the interplay of the three terms ΔE_{orb}, ΔE_{Pauli}, and ΔE_{elstat} that determines the bond energies and equilibrium distances of covalently bonded molecules. Molecules like N_2 and O_2, which are usually considered as covalently bonded, would not be bonded without the quasiclassical attraction ΔE_{elstat}.

Keywords: bond energy · bond theory · density functional calculations · energy decomposition analysis · main group elements

Introduction

The present understanding of chemical bonding considers ionic interactions and covalent bonding as two fundamental models for the chemical bond. Ionic bonds are generally discussed in terms of classical electrostatic interactions between point charges. Covalent bonding is usually introduced in terms of attractive orbital interactions between singly filled orbitals (electron-sharing bond) or between doubly occupied and vacant orbitals (donor–acceptor bond). Both bonding models neglect repulsive interactions between electrons having the same spin, although Pauli repulsion is stronger than electrostatic repulsion when orbital overlap becomes significantly large. It is only at very short internuclear distances that the electrostatic repulsion dominates the interatomic interactions. A bonding model that considers only Pauli repulsion as the crucial factor for determining molecular geometries is the valence shell electron pair repulsion (VSEPR) scheme.[1] Although we do not agree with all statements that were made in conjunction with the VSEPR model,[2] we accede to the conclusion that Pauli re-

[a] Dipl.-Chem. A. Krapp, Prof. G. Frenking
Fachbereich Chemie, Philipps-Universität Marburg
Hans-Meerwein-Strasse, 35043 Marburg (Germany)
Fax: (+49) 6421-282-5566
E-mail: Frenking@chemie.uni-marburg.de

[b] Dr. F. M. Bickelhaupt
Afdeling Theoretische Chemie
Scheikundig Laboratorium der Vrije Universiteit
De Boelelaan 1083, 1081 HV Amsterdam (The Netherlands)
Fax: (+31) 205-987-629
E-mail: FM.Bickelhaupt@few.vu.nl

Supporting information for this article is available on the WWW under http://www.chemeurj.org/ or from the author.

pulsion is a very important energy term for understanding chemical bonding. It was shown in numerous investigations by us in recent years that Pauli repulsion plays a pivotal role for bond energies and geometries of molecules.[3,4]

Another important concept for classifying chemical bonds is the division of orbital interactions into σ, π, and δ contributions, which are frequently associated with single (σ) and multiple (π, δ) bonding.[5] Hückel's recognition of the difference between σ and π bonding in his analysis of the chemical bonding in ethylene[6] was the starting point for his epochal study on chemical bonding in benzene.[7] The work was inspired by a theoretical study of the $^3\Sigma_g^-$ ground state of O_2 published earlier by Lennard-Jones.[8] Although the model of two different types of carbon–carbon bonds in ethylene was strongly opposed by Pauling,[9] it became a cornerstone for the interpretation of multiple bonds in main-group compounds. A characteristic difference between the two bonds is the overlap of the σ and π orbitals of two atoms or fragments E as a function of the internuclear distance r(E–E). Figure 1a illustrates the difference between σ and π bonding for an unspecified sp^x hybridized σ model orbital as is introduced in most chemistry textbooks.

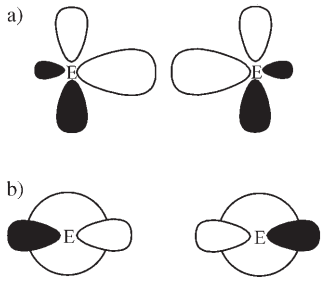

Figure 1. a) Schematic representation of bonding overlap between two sp^x hybrid orbitals. b) Schematic representation of bonding overlap between p(σ) and s orbitals.

The onset of σ bonding occurs at a longer E–E distance than the onset of π bonding. This is because the overlap of the sp^x-hybridized σ atomic orbitals (AOs), which are aligned along the internuclear axis, starts earlier than the overlap of the π orbitals, which are orthogonal to the σ bonding. The overlap of the σ orbitals $S(\sigma)$ has a maximum value at a certain distance r(E–E), while at shorter distances $S(\sigma)$ becomes smaller. One reason is that the bigger lobes of the sp^x hybrids do not overlap so well anymore. But, more importantly, the bigger lobes cross the nodal surface and begin to overlap with the smaller lobes of opposite sign at the backside of the other atom, which leads to cancellation of overlap (destructive interference).[10] Consequently, for two atoms or molecular fragments approaching each other, maximum σ(sp^x) overlap and associated bonding occur at some value of $r(\mathrm{E–E}) > 0$. Below this distance, the σ overlap, and thus the associated σ bonding, decreases again. In contrast, π bonding, which arises from the overlap and interaction of p(π), orbitals achieves its maximum strength when the internuclear distance becomes zero, at which $S(\pi) = 1$. This effect contributes to the well-known fact that double and triple bonds, which have σ and π contributions, are usually shorter than single bonds between the same atoms.

The above details may lead to the assumption that σ bonds achieve strongest attraction where $S(\sigma)$ is a maximum, and that further shortening attenuates the attraction because the overlap of the σ orbitals becomes smaller. The equilibrium bond length of a σ bond should then coincide with the distance where $S(\sigma)$ achieves its largest value. Multiple bonds, which have σ and π components, become somewhat shorter than σ bonds because the additional π bonding compensates for weaker σ interactions. This is the standard model for covalent bonding which rests on the assumption that bond strength correlates with orbital overlap.

Two important points are neglected in the above standard description of σ and π bonding. One point concerns the overlap of the σ orbitals as a function of the distance r(E–E). The s and p components of the sp^x hybridized σ orbital have a qualitatively different behavior when $S(\sigma)$ becomes small (see Figure 1b). The overlap of the s orbitals actually becomes $S(\mathrm{s}) = 1$ when $r(\mathrm{E–E}) = 0$, that is, it behaves like the overlap of p(π) orbitals. From this one would expect that interacting fragments with three valence electrons like boron atoms in B_2 should have a very short bond in which the six valence electrons occupy one 2s+2s σ orbital and a degenerate 2p(π)+2p(π) π orbital. This yields a singlet ($^1\Sigma_g^+$) electronic state with the configuration $(2\sigma_g)^2(1\pi)^4$. However, diatomic B_2 has a triplet ($X^3\Sigma_g^-$) ground state with two occupied σ orbitals, a doubly occupied degenerate π orbital, and a rather long B–B bond (1.590 Å).[11] The aforementioned $^1\Sigma_g^+$ state is a theoretically predicted, high-lying excited state.[12] Its bond length (1.416 Å)[11] is indeed shorter than that of the $X^3\Sigma_g^-$ triplet ground state, but not as short as the orbital overlap suggests. It is sometimes stated that nuclear–nuclear repulsion prevents shorter bond lengths. However, this is only true at interatomic distances well below the equilibrium bond length. It has been shown that the classical electrostatic interaction between two atoms nearly always favors shorter bonds than in the actual equilibrium structure, but is opposed by the Pauli repulsion.[3c,d,4b,13,20a] The notable exception is H_2, in which no Pauli repulsion is possible and thus a very short equilibrium bond length results at which the bonding orbital interactions are balanced by nuclear–nuclear repulsion.

The second important factor that is neglected in the above consideration is the Pauli repulsion between electrons having the same spin. It will be shown here that neither diminishing orbital overlap nor electrostatic interactions but Pauli repulsion prevents further shortening of the interatomic distances r(E–E). The lowest lying valence AO of any element is the (n)s orbital. As soon as there is more than one electron in the valence shell, the (n)s orbital becomes doubly occupied. The interaction between two atoms with doubly occupied (n)s orbitals is strongly repulsive due to the exclusion principle acting on the electrons on either atom that have the same spin. Since attractive interactions due to orbital mixing between occupied and vacant orbitals and Pauli repulsion are both functions of the orbital overlap, it

is a priori not clear at which size of the overlap maximum bonding takes place. It is important to recognize, however, that the onset of significant Pauli repulsion occurs at shorter interatomic distances than attractive orbital interactions, because occupied orbitals are more compact than vacant orbitals.

In this paper we report on an energy decomposition analysis (EDA) of the diatomic molecules E_2 of the first and second octal rows of the periodic table Li_2–F_2 and Na_2–Cl_2. We analyze the changes in the various energy contributions to the interaction energy as a function of the internuclear distances r(E–E). The emerging trends are compared with the nature and behavior of the orbital overlap between the atoms. Our quantitative bonding analysis contributes to the understanding of the chemical bond. In particular, they uncover how the interplay of electrostatic interaction, orbital interaction, and Pauli repulsion determines the strength and length of a series of archetypal single, double, and triple bonds in diatomic molecules.

The partitioning of the interaction energy into the three terms electrostatic interaction, orbital interaction, and Pauli repulsion might be criticized as arbitrary. The justification for the approach lies in the usefulness for the interpretation of the chemical bonds in terms of classical bonding models (covalent and electrostatic bonding, single and multiple bonds). The EDA makes it possible to assign data to the terms that are calculated at high levels of theory. The EDA thus serves as a bridge between the heuristic bonding models of chemistry that were developed in the pre-quantum chemistry era before 1927[10] and the physical mechanism that leads to a chemical bond.[14] The criticism of arbitrariness applies for *all* bonding models.[15] The value of a model lies in the scope of its applicability and its usefulness for chemical problems. A particular strength of the EDA is that it considers the total interatomic interactions that lead to the experimentally measurable bond dissociation energy and not only a particular fraction of the bond. For conceptual reasons, we sometimes distinguish in our paper between quasiclassical interactions (electrostatic term) and quantum theoretical interactions (sum of Pauli term and attractive orbital term). We do this in order to show that in many cases the molecules would be unbound if only the latter interactions are considered.

Computational Methods

The bond lengths of the diatomic molecules were optimized with the generalized gradient approximation (GGA) to density functional theory (DFT) by using the exchange functional of Becke[16] in conjunction with the correlation functional of Perdew[17] (BP86). Uncontracted Slater-type orbitals (STOs) were employed as basis functions for the SCF calculations.[18] The basis sets have triple-ζ quality augmented by two sets of polarization functions, that is, 2p and 3d functions on hydrogen and 3d and 4f functions on the other atoms. Core electrons (i.e., 1s for second- and 1s2s2p for third-period atoms) were treated by the frozen-core approximation. This level of theory is denoted BP86/TZ2P. An auxiliary set of s, p, d, f, and g STOs was used to fit the molecular densities and to represent the Coulomb and exchange potentials accurately in each SCF cycle.[19] The calculations were carried out with the program package ADF.[20]

The interatomic interactions were analyzed by means of an energy decomposition scheme that was developed independently by Morokuma[21] and by Ziegler and Rauk.[22] The focus of the bonding analysis is the instantaneous interaction energy ΔE_{int} of a bond A–B between two fragments A and B in the particular electronic reference state and in the frozen geometry of AB. In the present case of diatomic molecules E_2, ΔE_{int} is the energy difference between E_2 and the E atoms in the electronic reference state, which is in most cases the electronic ground state (see below). The interaction energy is divided into three main components [Eq. (1)].

$$\Delta E_{int} = \Delta E_{elstat} + \Delta E_{Pauli} + \Delta E_{orb} \quad (1)$$

The term ΔE_{elstat} corresponds to the classical electrostatic interaction between the unperturbed charge distributions of the prepared atoms and is usually attractive (vide infra). The Pauli repulsion ΔE_{Pauli} arises as the energy change associated with the transformation from the superposition of the unperturbed electron densities $\rho_{E(\alpha)}+\rho_{E(\beta)}$ of the isolated atoms to the wavefunction $\Psi^0 = N\hat{A}[\Psi_{E(\alpha)}\Psi_{E(\beta)}]$, which properly obeys the Pauli principle through explicit antisymmetrization ($\hat{A}$ operator) and renormalization (N = constant) of the product wavefunction.[20a] It comprises the destabilizing interactions between electrons on either atom of the same spin. The orbital interaction ΔE_{orb} accounts for charge transfer (i.e., donor–acceptor interactions between occupied orbitals on one moiety and unoccupied orbitals of the other, including the HOMO–LUMO interactions), polarization (empty/occupied orbital mixing on one fragment due to the presence of another fragment), and electron-pair bonding (the stabilization arising from the formation of the electron-pair bonding configuration in which the bonding combination between the SOMOs is formed and doubly occupied).[23] The ΔE_{orb} term can be decomposed into contributions from each irreducible representation of the point group of the interacting system. This makes it possible to quantitatively estimate the intrinsic strength of orbital interactions from orbitals having σ, π, δ, etc. symmetry.

For molecules in which the fragments do not electronically or geometrically relax after bond breaking, the interaction energy ΔE_{int} gives directly (by definition with opposite sign) the bond dissociation energy (BDE) D_e. If the two fragments of the chemical bond are in an electronically excited state or if they have more than one atom, which means that relaxation of the fragments occurs during bond rupture into the equilibrium geometry, the preparation energy ΔE_{prep} must be added to ΔE_{int} to obtain the bond dissociation energy [Eq. (2)].

$$\Delta E(=-D_e) = \Delta E_{int} + \Delta E_{prep} \quad (2)$$

Because the atomic fragments that were used in our calculations are in the electronic ground state, it follows that for the E_2 molecules $\Delta E_{prep}=0$ and $\Delta E_{int}=-D_e$. For technical reasons, the EDAs involving open-shell fragments neglect the spin polarization in the fragments and thus yield slightly too stable bonds (on the order of a few kcal mol^{-1} per unpaired electron). The bond energies were corrected for the spin-polarization error ΔE_{corr}, which is given in the tables. Further details on the EDA can be found in the literature.[20]

Finally we comment on the calculated values for the energies, which are presented to two decimal places. This is not because there is chemical significance in the figures after the decimal point, but to guarantee that the data can be correctly reproduced.

Results and Discussion

Interaction of two electrons: It is instructive for the remainder of the paper to consider the interactions between two

electrons as a function of their distance r_{12}. Figure 2 (left) shows three calculated curves for electron–electron (e–e) repulsion. The dashed curve gives the calculated values from Coulomb's law of electrostatic interaction between two equal point charges q [Eq. (3)].

$$\Delta E_{\mathrm{elstat}}(\mathrm{classical}) = q_1 q_2 / r_{12} \tag{3}$$

The curve shows the well-known behavior of the repulsion of two point charges, which approaches an infinite value when $r=0$. The second dotted curve results from the correct equation for the repulsion between two electrons, described by a wave function χ rather than by a point charge q. We chose a 1s hydrogen AO ($\xi=1.0$) for the calculation. From the wave function χ one obtains the charge density ρ from Equation (4a). The quasiclassical repulsion between two electrons is then given by Equation (4b) in which τ_1 and τ_2 are the coordinates of electrons 1 and 2, respectively.

$$\rho = |\chi|^2 \tag{4a}$$

$$\Delta E_{\mathrm{elstat}} = \int \rho_1 \rho_2 / r_{12} \mathrm{d}\tau_1 \mathrm{d}\tau_2 \tag{4b}$$

There are two important differences between the repulsive curves given by Equations (3) and (4b). One difference is that the repulsion calculated by Equation (4b) gives a finite value when $r=0$. This is known from classical electrostatics and from bonding models of MO theory where two electrons with opposite spin occupy the same spatial orbital. The second difference concerns the shape of the curves in the region between 1 and 2 Å in which most chemical bonds between lighter atoms have their equilibrium value. The two curves calculated by Equations (3) and (4b) are nearly indistinguishable at large distances r, but starting at about 2 Å, the electrostatic repulsion given by Equation (4b) is less than the classical repulsion between two point charges. This is very important for understanding the electrostatic interactions between two neutral atoms in a molecule.

It is often assumed that classical electrostatic interactions between two neutral atoms neglecting orbital mixing yield only weak attraction or even repulsion, and that orbital interactions are required to obtain chemical bonding. The assumption is not correct! It was already pointed out in 1974 by Hirshfeld and Rzotkiewicz[13b] and in 1986 by Spackman and Maslen[13a] that the classical electrostatic interaction between two neutral atoms at equilibrium distance is strongly attractive when Equation (4b) is used for the electron–electron interaction except for H_2. Since the electron density which is used in Equation (4b) comes from a quantum chemical calculation, the calculated interaction is named quasiclassical.[24] Recently, it was shown that many nonpolar bonds of diatomic and larger molecules which are typical examples for covalent bonding have strongly attractive contributions from $\Delta E_{\mathrm{elstat}}$.[3c] A mathematical explanation for the finding was given by Kutzelnigg[25] and by Bickelhaupt and Baerends.[20a] Figure 2 illustrates the mathematical reasoning.

The actual electron–electron repulsion in the region of chemical bonding $r<2$ Å shown in Figure 2 (left) is less

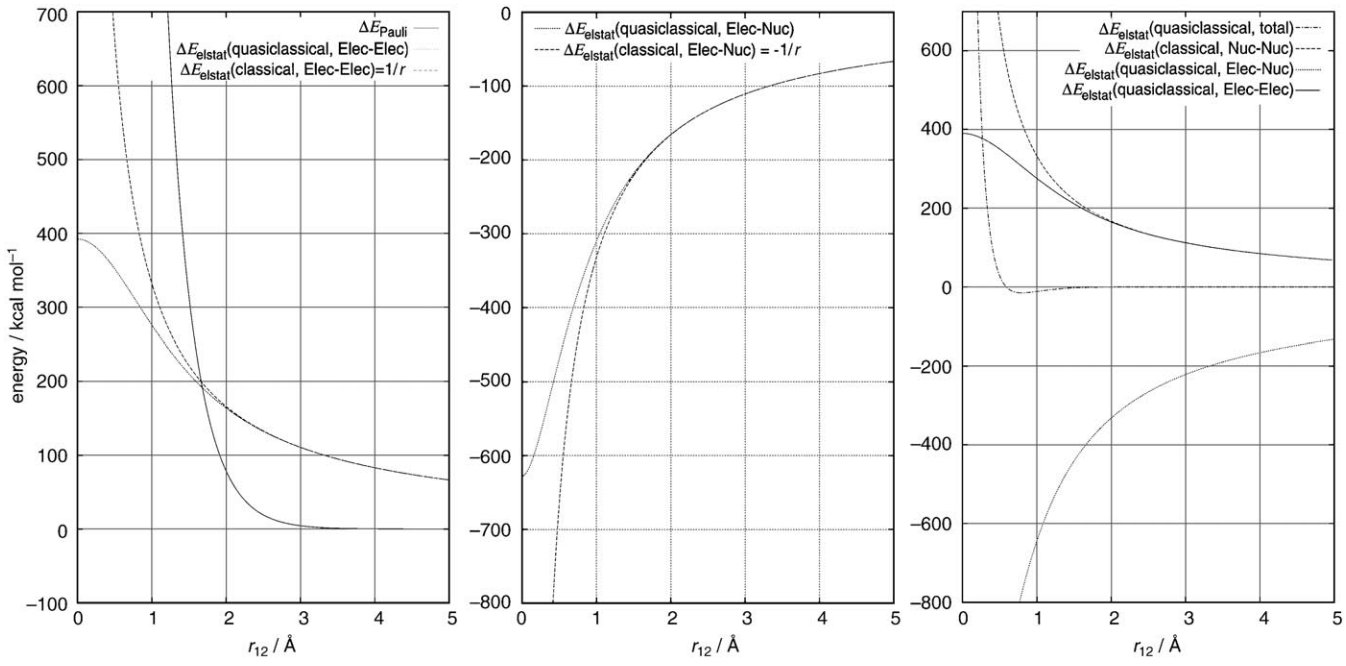

Figure 2. Calculated interaction energies between two charged particles as a function of their distance r_{12}. Left: Repulsive interactions between two electrons calculated classically $\Delta E_{\mathrm{elstat}}(\mathrm{classical}) = q_1 \times q_2 / r_{12}$ (dashed line); quasiclassical repulsion between two electrons in 1s orbitals $\Delta E_{\mathrm{elstat}} = \int \rho_1 \rho_2 / r_{12} \mathrm{d}\tau_1 \mathrm{d}\tau_2$ (dotted line); exchange repulsion between two electrons with the same spin in 1s orbitals $\Delta E_{\mathrm{Pauli}}$ (solid line). Middle: Attractive interactions between proton and electron calculated classically $\Delta E_{\mathrm{elstat}}(\mathrm{classical}) = -q_1 \times q_2 / r_{12}$ (dashed line); quasiclassical attraction between proton and electron in a 1s orbital $\Delta E_{\mathrm{elstat}} = -q_1 \int \rho_2 / r_{12} \mathrm{d}\tau_2$ (dotted line). Right: Sum of the above repulsive and attractive quasiclassical interaction in H_2.

than what is calculated by the point-charge approximation using Equation (3). This has important implications for interatomic electrostatic interactions. Since the actual electron–electron repulsion at equilibrium distance is weaker than that calculated by using Equation (3), the net electrostatic interaction between neutral atoms would become attractive if the point-charge approximation were valid for the remaining terms. This is the case for the nuclear–nuclear repulsion, because the spatial extension of the nuclei can be neglected for chemical interactions.

What about nuclear–electron attraction? Figure 2 (middle) shows curves for the electrostatic attraction calculated classically between two point charges of opposite sign and quasiclassically for the attraction between a positive point charge q_1 and a negative charge ρ_2 of one electron in a 1s hydrogen orbital [Eq. (5)].

$$\Delta E_{\text{elstat}} = -q_1 \int \rho_2 / r_{12} \mathrm{d}\tau_2 \qquad (5)$$

The two curves begin to diverge at a distance $r \approx 1.5$ Å, which is later than for the two curves for the electrostatic repulsion shown in Figure 2 (left). The difference in diverging behavior becomes evident when the final values for the quasiclassical attraction and repulsion at $r(\mathrm{E{-}E}) = 0$ Å are compared. The nuclear–electron (N–e) attraction becomes -627.5 kcal mol^{-1}, which is the electrostatic attraction in a hydrogen atom, while the e–e repulsion becomes 392.2 kcal mol^{-1}. Note that the former value is obtained from the interaction of one electron, while the latter comes from the interaction of two electrons. The quasiclassical interaction between two atoms will become attractive when the deviation of the e–e repulsion from the point-charge value becomes larger than twice the deviation of the N–e attraction from the classical value. This is shown in Figure 2 (right) in which addition of the quasiclassical attraction and repulsion gives a minimum at 0.98 Å with a well depth of 12.3 kcal mol^{-1}.

The third curve in Figure 2 (left), denoted ΔE_{Pauli}, was calculated to demonstrate the specific interactions between two electrons that have the same spin. The quantum theoretical Pauli postulate requires that two electrons with the same spin cannot occupy the same spatial region. The interactions between two electrons with the same spin are therefore not only determined by Equation (4b), which describes the electrostatic repulsion. To fulfill the Pauli postulate, the product wave function of two electrons must be antisymmetric with respect to coordinate transformation. Figure 2 (left) shows that the antisymmetrization of the product wave function $\chi_1\chi_2$ changes the energy at longer interelectronic distances very little. The onset of ΔE_{Pauli} is at about 3 Å. At distances $r < 2$ Å the increase of ΔE_{Pauli} becomes very steep. This is the same region where the two curves for the electron–electron repulsion describing the classical and the quantum theoretical behavior begin to diverge. It is important to recognize that, in the bonding region between 1–2 Å, ΔE_{Pauli} increases much more sharply than ΔE_{elstat}. Moreover, as mentioned above, the overall electrostatic interaction in most molecules is attractive. Thus, the crucial term which yields repulsive interactions in the bonding region of 1–2 Å, except for two-electron systems such as H_2, is the Pauli term ΔE_{Pauli}.

Note that the energy minimum shown in Figure 2 (right) comes from only two electrons interacting with two nuclei of charge $Z = +1$. It is shown below that the quasiclassical interaction between heavier atoms in most cases becomes much more attractive than in H_2. Already in Be_2, which has only filled s-type orbitals like dihydrogen, but a nuclear charge of $Z = +4$, the ΔE_{elstat} term becomes attractive by -17.87 kcal mol^{-1}, which is larger than the total bond dissociation energy. Besides the nuclear charge, the size of the orbitals of the interacting electrons determines the strength of the electron–electron and nucleus–electron interactions. Electrons in compact orbitals behave more like point-charges yielding stronger interatomic electron–electron repulsion and nucleus–electron attraction than electrons in diffuse orbitals. The divergent behavior of the quasiclassical electrostatic interaction from the point-charge interaction shown in Figure 2 (left and middle) will already occur at longer distances when the electrons are in (n)s orbitals for which $n > 1$. Another very important factor which determines the electrostatic interactions is the shape of the orbitals (Figure 3).

Figure 3 (left) gives curves for the electrostatic repulsion between electrons which are in 2s or 2p AOs ($\xi = 1.0$). Clearly, at any finite interelectronic distance, 2p(σ)–2p(σ) repulsion (green full line) is stronger than 2s–2s repulsion (red full line). At distances r greater than about 1.9 Å it is even stronger than the classical repulsion between two point charges (black full line). The 2p(π)–2p(π) repulsion (blue full line) is weaker than 2s–2s repulsion at finite distances r greater than about 1.0 Å at which the two lines cross. At short distances the 2p(π)–2p(π) repulsion approaches the value of the 2p(σ)–2p(σ) repulsion and the two curves converge when $r = 0$. The electrostatic repulsion 2p(π)–2p′(π) between electrons in orthogonal p(π) orbitals (blue dotted line) is weaker at finite distances than all other repulsions. The 2p(σ)–2p(π) repulsion (green dotted line) is stronger than the 2s–2s repulsion at finite distances r greater than about 0.7 Å, at which the two lines cross before the former repulsion approaches the value of 2p(π)–2p′(π). The curves for 2s–2p(σ) repulsion (red dotted line) and 2s–2p(π) repulsion (red dashed line) are intermediate between the 2p(σ)–2p(σ) and 2s–2s repulsions. They converge to the latter curve at $r = 0$ Å. It follows that the shape of the occupied orbital significantly influences the strength of the electron–electron repulsion.

The same conclusion can be drawn from the results for the nucleus–electron attraction where the electron is in a 2s, 2p(σ), or 2p(π) AO. The calculated curves for a nucleus N with a charge $Z = +1$ are shown in Figure 3 (middle). At all finite distances N–2p(σ) attraction is stronger than N–2s attraction, but the former interaction has a minimum of -344.9 kcal mol^{-1} at $r = 0.58$ Å before it approaches its limiting value of -318.8 kcal mol^{-1} at $r = 0$ Å. The curve for the N–2p(π) attraction does not have such a minimum. This in-

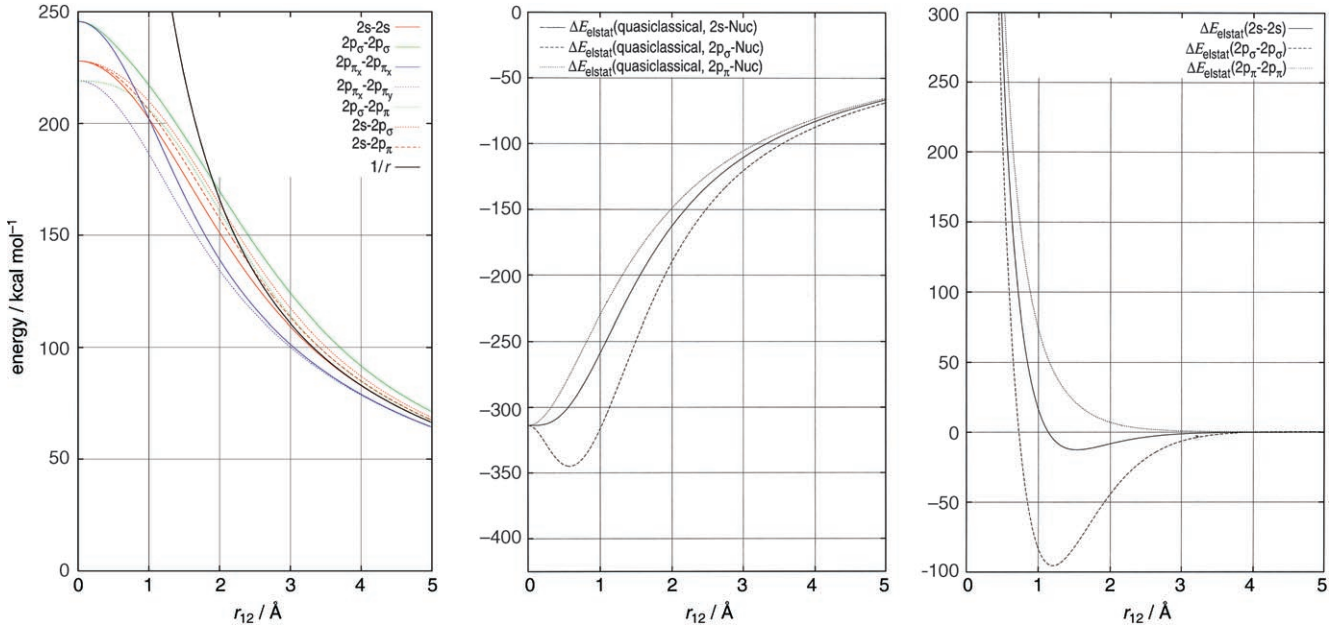

Figure 3. Calculated attraction and repulsion between two charged species as in Figure 2 with the electron in a 2s or 2p orbital. Left: Classical repulsion between two point charges $\Delta E_{\text{elstat}}(\text{classical}) = q_1 q_2 / r_{12}$ (black full line); quasiclassical repulsion between two electrons $\Delta E_{\text{elstat}} = \int \rho_1 \rho_2 / r_{12} \mathrm{d}\tau_1 \mathrm{d}\tau_2$ in orbitals: 2s–2s (red full line); 2p(σ)–2p(σ) (green full line); 2p(π)–2p(π) (blue full line); 2p(σ)–2p(π) (green dotted line); 2p(π)–2p′(π) (blue dotted line); 2s–2p(σ) (red dotted line); 2s–2p(π) (red dashed line). Middle: Quasiclassical attraction between proton and electron $\Delta E_{\text{elstat}} = -q_1 \int \rho_2 / r_{12} \mathrm{d}\tau_2$ for N–2s (solid line); N–2p(σ) (dashed line); N–2p(π) (dotted line). Right: Sum of the quasiclassical attractive and repulsive interactions in a model two-electron diatomic molecule with nuclear point charges $Z = +1$. The electrons are in 2s orbitals (solid line); 2p(σ) orbitals (dashed line); 2p(π) orbitals (dotted line).

teraction is weaker than the N–2s and N–2p(σ) attractions at all finite distances.

Figure 3 (right) shows three curves for the sum of the quasiclassical attractive and repulsive interactions in a diatomic molecule E_2 with nuclear charge $Z = +1$ in which the two electrons are in the above atomic orbitals. The curve for which the electrons are in 2p(π) AOs which are in the same plane does not have a minimum. The curve for the occupied 2s AO has a minimum at $r = 1.53$ Å with a well depth of -12.5 kcal mol^{-1}. A deep energy minimum of -95.6 kcal mol^{-1} at $r = 1.20$ Å is found when the electrons occupy a 2p(σ) AO. These last results explain why quasiclassical attraction may strongly contribute to the chemical bonding in nonpolar bonds between atoms which have sp^x-hybridized σ orbitals.[3]

Diatomic molecules Li_2–F_2: The EDA results for the diatomic molecules of the elements of the first octal row Li–F are given in Table 1. Figure 4 schematically shows the electron configuration and the orientation of the atoms with the

Table 1. Energy partitioning analysis of the first-row diatomics E_2 (E = Li–F) in C_{2v} at BP86/TZ2P (ZORA); energies in kcal mol^{-1}, distances r(E–E) in Å.

	Li	Be	B	C	N	O	F
El. state	$^1\Sigma_g^+$	$^1\Sigma_g^+$	$^3\Sigma_g^-$	$^1\Sigma_g^+$	$^1\Sigma_g^+$	$^3\Sigma_g^-$	$^1\Sigma_g^+$
ΔE_{int}	−20.71	−7.86	−74.67	−140.79	−240.23	−141.87	−52.87
ΔE_{Pauli}	1.76	41.62	135.00	252.20	802.37	464.93	146.07
ΔE_{elstat}[a]	−8.30 (36.9%)	−17.87 (36.1%)	−33.14 (15.8%)	−3.22 (0.8%)	−312.85 (30.0%)	−159.74 (26.3%)	−41.20 (20.7%)
ΔE_{orb}[a]	−14.17 (63.1%)	−31.62 (63.9%)	−176.53 (84.2%)	−389.77 (99.2%)	−729.76 (70.0%)	−447.07 (73.7%)	−157.75 (79.3%)
ΔE_{a1}[b] (σ)	−14.17	−31.62	−104.50 (59.2%)	−201.74 (51.8%)	−478.81 (65.6%)	−319.48 (71.5%)	−151.49 (96.0%)
ΔE_{a2}[b] (δ)	0.00	0.00	0.00	0.00	0.00	0.0	0.00
ΔE_{b1}[b] (π)	0.00	0.00	−36.02 (20.4%)	−94.02 (24.1%)	−125.47 (17.2%)	−59.11 (13.2%)	−3.13 (2.0%)
ΔE_{b2}[b] (π)	0.00	0.00	−36.02 (20.4%)	−94.02 (24.1%)	−125.47 (17.2%)	−68.48 (15.3%)	−3.13 (2.0%)
$\Delta E_{\text{corr.}}$[e]	0.29	0.00	1.92	3.27	4.15	4.82	2.72
D_e[c]	20.42 (24.62)	7.86 (2.28; 2.70 [calcd])[d]	72.75 (71.15)	137.52 (145.86)	236.08 (228.43)	137.05 (120.23)	50.15 (38.25)
r(E–E)[c]	2.731 (2.673)	2.442 (2.45)[d]	1.617 (1.590)	1.253 (1.243)	1.102 (1.098)	1.224 (1.208)	1.420 (1.412)

[a] Values in parentheses are percentage contributions to the total attractive interactions $\Delta E_{\text{elstat}} + \Delta E_{\text{orb}}$. [b] Values in parentheses are percentage contributions to the total orbital interactions ΔE_{orb}. [c] Experimental values in parentheses from reference [11a] unless otherwise specified. [d] Experimental value for D_e and E–E: V. E. Bondybey, *Chem. Phys. Lett.* **1984**, *109*, 436; calculated value for D_e: J. M. L. Martin, *Chem. Phys. Lett.* **1999**, *303*, 399. [e] Correction for spin polarization.

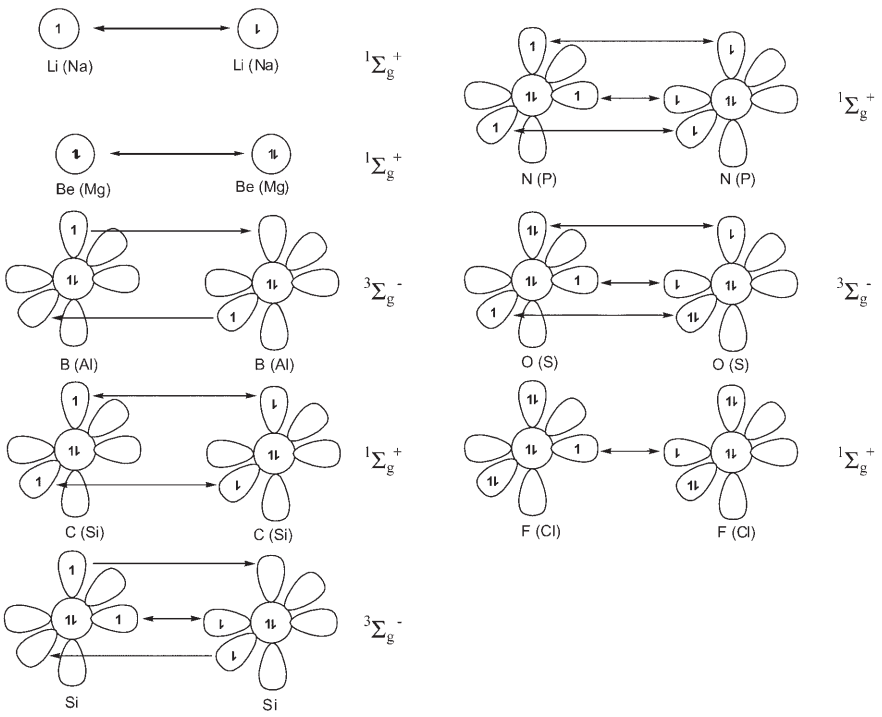

Figure 4. Schematic representation of the electron configuration and the orientation of the atoms with the chosen orbital populations for the EDA. Note that for the $^3\Sigma_g^-$ state of Si_2, O_2, and S_2 a spin change of one electron in a singly occupied p(π) orbital takes place in the EDA calculation.

chosen orbital populations.[26] We also present in Figure 5 an MO correlation diagram for formation of the molecular orbitals of E_2 from the atomic orbitals of E. The electronic

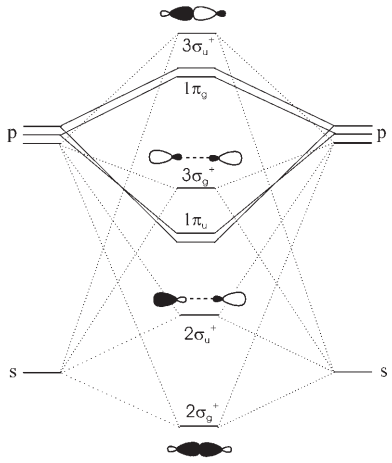

Figure 5. Orbital correlation diagram for diatomic molecules of main-group elements. The numbering of the orbitals is given with respect to the elements of the first octal row. For some systems the $3\sigma_g^+$ orbital lies lower in energy than the $1\pi_u$ MO.

states of the atoms that were chosen for the EDA (Figure 4) correlate with the symmetry-allowed formation of E_2 in the electronic ground state. This means that the electronic states of E in the EDA are the ground states. Note that the atomic fragments which are used in the EDA calculations of the ($^3\Sigma_g^-$) triplet states of O_2, Si_2, and S_2 are two atoms in the ^3P ground state, which are the symmetry-allowed dissociation products.[27] Hence, a spin change of one electron in a p(π) orbital must take place during the EDA calculation, because a triplet molecule is constructed from two triplet fragments. The two components of the π orbital interactions in the EDA therefore have slightly different values.

A comparison of the calculated bond lengths r(E–E) and bond dissociation energies D_e with the experimental values shows good agreement between the two sets of data. The theoretical bond dissociation energies of F_2 and N_2 are somewhat larger than the experimental values, but the agreement is still sufficient for the purpose of this work.

The EDA of Li_2 indicates that the attractive lithium–lithium interactions have about one-third electrostatic character, while about two-thirds come from the ΔE_{orb} term. The ΔE_{Pauli} value is very small, because there is only Pauli repulsion between core–core and core–valence electrons, but no valence–valence repulsion. Previous investigations suggested[25] that induction forces significantly contribute to the chemical bond in Li_2. We performed an EDA of Li_2 in which the p valence AOs and all polarization functions were deleted. This inhibits the polarization of the 2s valence orbital and thus eliminates induction. Table 2 gives the EDA result of Li_2 with the reduced orbital space. The ΔE_{orb} term drops from $-14.17\,kcal\,mol^{-1}$ to $-9.82\,kcal\,mol^{-1}$. The remaining part comes from genuine orbital interactions, while the difference of $-4.34\,kcal\,mol^{-1}$ is due to polarization and enhanced orbital interaction through hybridization. The EDA calculation of Li_2 in which also the higher order s functions are deleted gives $\Delta E_{orb} = -8.06\,kcal\,mol^{-1}$ (Table 2). The small difference of $-1.76\,kcal\,mol^{-1}$ to the ΔE_{orb} value for which the p and polarization functions are deleted indicates the energetic effect of mixing in the 3s (and higher) functions yielding a different radius for the Li valence s function in Li_2.

A peculiar feature of the two-electron bond in Li_2 is that removing one electron from the doubly occupied $2\sigma_g^+$ bonding orbital (Figure 5) strengthens the binding interactions. The BDE of Li_2^+ ($D_e = 33.2\,kcal\,mol^{-1}$) is higher than the BDE of Li_2 ($D_e = 24.6\,kcal\,mol^{-1}$).[11a] Table 2 gives the EDA results for Li_2^+. The data show that the higher bond energy of the cation is well reproduced at the BP86/TZ2P level.

Table 2. Energy partitioning analysis of some first-row dimers E_2 and related species at BP86/TZ2P using designated fragments. Energies in kcal mol^{-1}, distances r(E–E) in Å.

	Li_2[a] $^1\Sigma_g^+$	Li_2[a] $^1\Sigma_g^+$	Li_2^+ $^2\Sigma_g^+$	Li_2^+ $^2\Sigma_g^+$	Li_2^+ $^2\Sigma_g^+$	Be_2 $^1\Sigma_g^+$	Na_2 $^1\Sigma_g^+$	Na_2 $^1\Sigma_g^+$
Virtual space	only s orbitals in virtual space	no virtual orbitals	full	only s orbitals in virtual space	no virtual orbitals	only s orbitals in virtual space	only s orbitals in virtual space	no virtual orbitals
ΔE_{int}	−16.36	−14.60	−27.85	−14.91	−12.27	19.15	−15.18	−14.09
ΔE_{Pauli}	1.76	1.76	2.92	2.92	2.92	41.62	5.07	5.07
ΔE_{elstat}	−8.30	−8.30	+2.07	+2.07	+2.07	−17.87	−10.67	−10.67
ΔE_{orb}	−9.82	−8.06	−32.84	−19.89	−17.26	−4.60	−9.58	−8.49
ΔE_{a1} (σ)	−9.82	−8.06	−32.84	−19.89	−17.26	−4.60	−9.58	−8.49
ΔE_{a2} (δ)	0.00	0.00	0.00	0.00	0.00	0.00	0.00	0.00
ΔE_{b1} (π)	0.00	0.00	0.00	0.00	0.00	0.00	0.00	0.00
ΔE_{b2} (π)	0.00	0.00	0.00	0.00	0.00	0.00	0.00	0.00
ΔE_{corr}[b]			0.14					
D_e[a]			27.71(33.2)					
r(E–E)[a]			3.1105					

[a] Experimental values in parentheses from reference [11a]. [b] Correction for spin polarization.

The EDA data indicate that the stronger bond of Li_2^+ comes solely from the ΔE_{orb} term. The Pauli repulsions in Li_2 and Li_2^+ have nearly the same value, and the electrostatic interaction in Li_2^+ is even repulsive. Thus, Li_2^+ is besides H_2 one of the rare examples in which the classical electrostatic interaction at equilibrium distance is not attractive.[3c] We also performed an EDA of Li_2^+ in which the p valence AOs and the polarization functions were deleted. Table 2 shows that after deleting these orbitals the ΔE_{orb} term drops from −32.84 to −19.89 kcal mol^{-1}, which is, however, still stronger than in Li_2. This indicates that the stronger bond in Li_2^+ mainly comes from genuine orbital interactions in which the much lower lying 2s AOs of the cation significantly enhance the bonding. This is supported by the calculated ΔE_{orb} value of −17.26 kcal mol^{-1} after deleting the higher order (n)s orbitals ($n>2$) of Li in the EDA of Li_2^+ (Table 2). The difference to the previous value (−19.89 kcal mol^{-1}) suggests that the change in the 2s orbital radius through bond formation in Li_2^+ yields a stabilization of −2.63 kcal mol^{-1}, which is more than in Li_2.

Figure 6 (top) shows the orbital overlap of the valence s and p orbitals of Li_2 as a function of the distance r(Li–Li). Interestingly, at the equilibrium distance of Li_2, the sum of the overlap of the σ orbitals S(σ) reaches its maximum value. We think that this is a coincidence, because the dominant atomic orbital for the $2\sigma_g^+$ MO is the 2s AO. Figure 6 (bottom) shows that the attractive energy terms ΔE_{orb} and ΔE_{elstat} still further increase in absolute values when the equilibrium distances becomes up to about 0.5 Å shorter. The interatomic force that prevents a shorter bond than the equilibrium value is the Pauli repulsion. Figure 6 (bottom) shows that the upward slope of the ΔE_{Pauli} curve is larger than the downward slope of the ΔE_{orb} and ΔE_{elstat} curves. Note that ΔE_{Pauli} becomes negative at longer distances r(Li–Li). This unrealistic result comes from the self-interaction error (SIE) of the functionals used for the DFT calculations. There are no gradient-corrected DFT functionals known to us which avoid this error. Without the SIE, the ΔE_{Pauli}

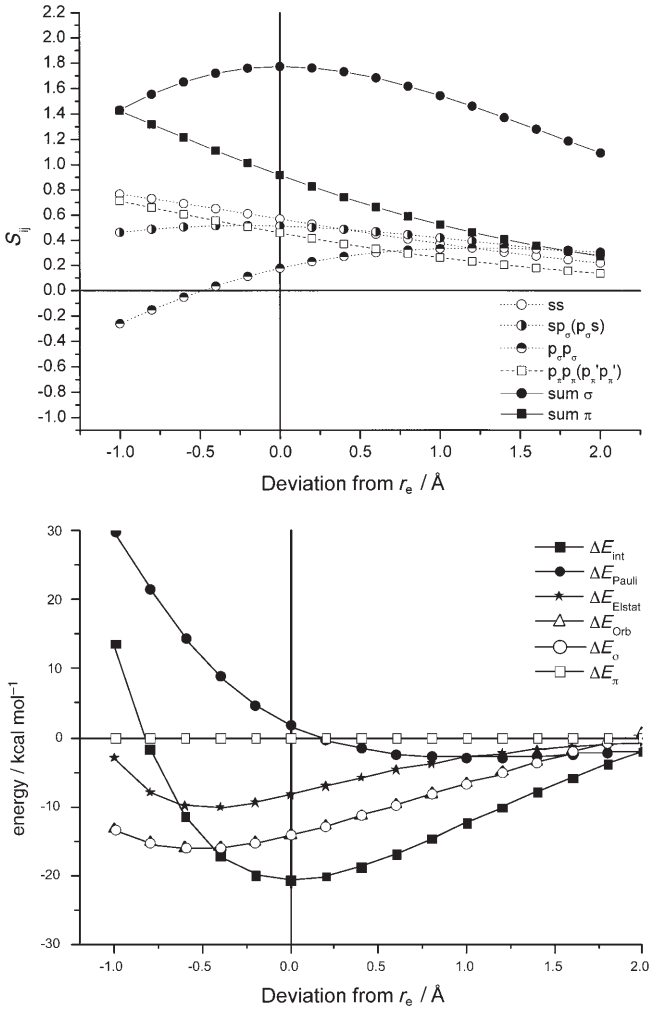

Figure 6. Top: Overlap integrals of the atomic 2s and 2p orbitals of Li_2 as a function of the interatomic interaction. Bottom: Calculated EDA values for Li_2 as a function of the interatomic distance. The reference value 0.0 is the calculated equilibrium bond length of 2.731 Å.

values would be slightly larger,[28] but the shape of the curves is not affected. Therefore, the error can be neglected.

Be_2 has only a very weak bond that is usually explained by occupation of the antibonding $2\sigma_g^-$ MO canceling the bonding contribution of the $2\sigma_g^+$ MO (Figure 5). The calculation on Be_2 ($^1\Sigma_g^+$) gave a BDE of only 7.86 kcal mol^{-1} (Table 1). The breakdown of the EDA into the three energy terms shows a significantly larger ΔE_{Pauli} value of 41.62 kcal mol^{-1} compared with Li_2 (1.76 kcal mol^{-1}). There is Pauli repulsion between the valence electrons in Be_2 that does not occur in Li_2. The ΔE_{orb} term contributes 31.62 kcal mol^{-1} (63.9%) to the attractive interactions. This comes mainly from the mixing of the 2p(σ) AO of Be into the $2\sigma_g^+$ and $2\sigma_g^-$ MOs, which enhances the bonding character of the former and weakens the antibonding character of the latter. This is further supported by a computational experiment in which we carried out an EDA of Be_2 in which the 2p valence orbitals and the polarization functions were deleted. Table 2 shows that ΔE_{orb} becomes dramatically smaller after deleting the empty orbitals. The strength of the remaining orbital interactions is only −4.60 kcal mol^{-1}, which comes from mixing of the 3s and higher order s functions with the valence orbitals.

We want to connect the information given by the EDA data in Table 1 and the qualitative MO diagram shown in Figure 5. It seems surprising that the ΔE_{orb} term gives stabilizing values for Be_2, while the MO diagram suggests that the orbital interactions should be weakly repulsive. The repulsion which comes from the antibonding combination of the 2s AOs yielding the $2\sigma_g^-$ MO is included in the ΔE_{Pauli} term. This is because the molecular wave function becomes antisymmetrized when ΔE_{Pauli} is determined, which leads to molecular orbitals having the symmetry shown in Figure 5. The stabilizing contribution of the ΔE_{orb} term then comes from the relaxation of the antisymmetrized wave function toward the final SCF solution.

Figure 7 gives the orbital overlaps and the EDA results for Be_2 at different bond lengths. The maximum overlap $S(\sigma)$ is reached at a distance which is about 0.5 Å shorter than the equilibrium value (Figure 7 top). The stabilizing contribution of the orbital interactions further increases at shorter bond lengths far below the equilibrium distance (Figure 7 bottom). The ΔE_{orb} term remains more stabilizing than ΔE_{elstat} at all interatomic distances which are shown. This comes mainly from the mixing of the 2p(σ) orbital with the 2s AO, which enhances the orbital interactions and polarization of the electronic charge. The stronger orbital interactions and electrostatic attraction at shorter distances are compensated by the Pauli repulsion. Note that the absolute value for ΔE_{Pauli} at r_e is larger than ΔE_{orb}. This means that the quantum theoretical terms ΔE_{orb} and ΔE_{Pauli} do not yield an energy minimum for Be_2. Without the quasiclassical electrostatic attraction ΔE_{elstat} diberyllium would not be a stable species. As noted in the introduction, this is *not* because the Be atom has a closed-shell electron configuration. The same situation can be found when atoms or fragments with unpaired electrons interact. Examples are given below.

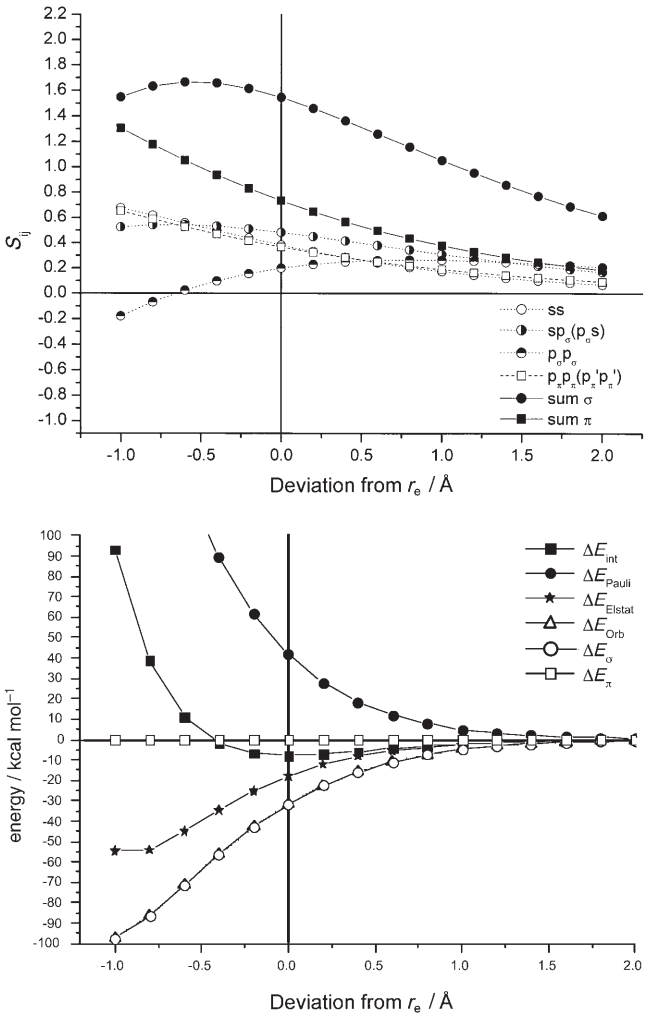

Figure 7. Top: Overlap integrals of the atomic 2s and 2p orbitals of Be_2 as a function of the interatomic interaction. Bottom: Calculated EDA values for Be_2 as a function of the interatomic distance. The reference value 0.0 is the calculated equilibrium bond length of 2.442 Å.

Diatomic B_2 has a triplet ($X^3\Sigma_g^-$) ground state in which two electrons occupy the degenerate $1\pi_u$ orbital (Figure 5). The EDA data in Table 1 show that the π contribution to the total orbital interactions accounts for −72.04 kcal mol^{-1}, which is 40.8% of ΔE_{orb}. The σ orbital interactions add −104.50 kcal mol^{-1} to the ΔE_{orb} term. Since the Pauli repulsion ΔE_{Pauli} = 135.00 kcal mol^{-1} comes only from σ electrons the total σ interaction from $\Delta E_{orb} + \Delta E_{Pauli}$ is repulsive by 30.50 kcal mol^{-1}. The net bonding comes from the stabilizing contributions of $\Delta E(\pi)$ (−72.04 kcal mol^{-1}) and ΔE_{elstat} (−33.14 kcal mol^{-1}). Thus, chemical bonding in B_2 has nearly equally strong contributions from the quantum theoretical terms $\Delta E_{orb} + \Delta E_{Pauli}$ (−41.54 kcal mol^{-1}) and from the quasiclassical term ΔE_{elstat} (−33.14 kcal mol^{-1}). We note that ΔE_{Pauli} in B_2 is significantly larger (135.00 kcal mol^{-1}) than in Be_2 (41.62 kcal mol^{-1}), which can be explained by the sharp increase of the Pauli repulsion at interatomic distances shorter than 2 Å (see Figure 2 left). B_2 has a much shorter bond (1.617 Å) than Be_2 (2.442 Å). The EDA data for the σ

interactions ($\Delta E_{a1}+\Delta E_{Pauli}$) and π interactions ($\Delta E_{b1}+\Delta E_{b2}$) suggest that B_2 is a π-bonded molecule. This is in agreement with the qualitative MO correlation diagram shown in Figure 5.

Figure 8 shows the trend of the orbital overlaps and the EDA results for B_2 at different distances *r*. The maximum value for $S(\sigma)$ is not found at the B–B equilibrium distance

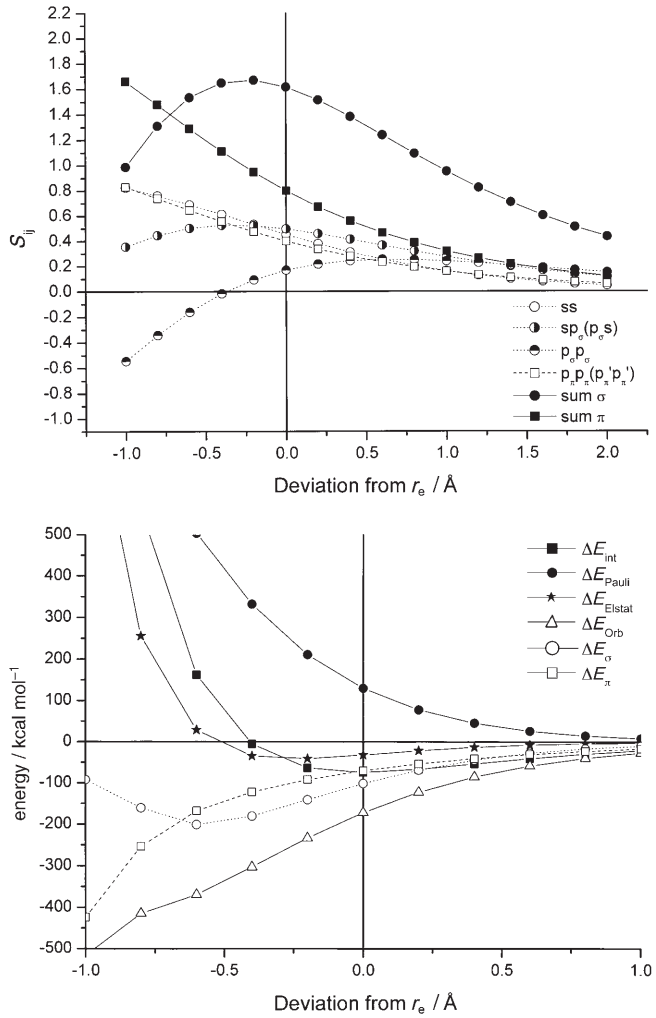

Figure 8. Top: Overlap integrals of the atomic 2s and 2p orbitals of B_2 as a function of the interatomic interaction. Bottom: Calculated EDA values for B_2 as a function of the interatomic distance. The reference value 0.0 is the calculated equilibrium bond length of 1.617 Å.

(Figure 8 top). The overlap of the σ orbitals increases at shorter distances and reaches its largest value about 0.25 Å below the calculated bond length. Inspection of Figure 8 (bottom) shows that the reason for the longer equilibrium distance is the Pauli repulsion. Note that the strength of the attractive σ orbital interactions reaches its maximum about 0.7 Å below r_e for which ΔE_{elstat} is already repulsive.

Diatomic C_2 has a singlet ($X^1\Sigma_g^+$) ground state in which four electrons occupy the degenerate $1\pi_u$ orbital (Figure 5). According to the qualitative MO model, C_2 has two π bonds but no σ bond. Table 1 shows that the Pauli repulsion in C_2 is nearly twice as strong as in B_2 (252.20 kcal mol^{-1}) and outweighs the attractive σ orbital interactions (−201.74 kcal mol^{-1}). The large value of ΔE_{Pauli} can be explained by the shorter equilibrium bond length of C_2 (1.253 Å) compared with B_2 (1.617 Å). The Pauli repulsion in C_2 comes exclusively from electrons in σ orbitals. Hence, the total σ contribution of $\Delta E_{orb}+\Delta E_{Pauli}$ is repulsive, which is in agreement with the qualitative MO model (Figure 5). The strength of the π bonding is −188.04 kcal mol^{-1}, which is sufficient to compensate the repulsive σ interactions. Like B_2, C_2 is a π-bonded molecule. A peculiar feature of dicarbon is the unusually weak calculated electrostatic attraction. Although the C–C bond is rather short, the ΔE_{elstat} term contributes only −3.22 kcal mol^{-1} to the binding, which is the smallest value of all E_2 molecules investigated here. Note that the electrostatic interactions come from electrons in carbon s and p(π) orbitals, which are much more compact than for boron. It was shown above (see Figure 3 right) that electrons in 2s orbitals yield only small attraction, while electrons in 2p(π) AOs yield repulsion. The reason for the weak electrostatic component in C_2 and the trend in E_2 is discussed in more detail below.

The correlation curves of the orbital overlaps and the EDA data at different interatomic distances for C_2 (Figure 9) show a similar behavior to those of B_2 (Figure 8). The maximum of the σ overlap appears in both cases at a distance that is about 0.25 Å shorter than the equilibrium value. It is the increase in ΔE_{Pauli} that prevents shorter bonds as $S(\sigma)$ reaches its maximum. The most striking result shown in Figure 9 (bottom) is the curve for ΔE_{elstat}, which at no distance attains a significantly attractive value.

The MO diagram for N_2 indicates (Figure 5) that the molecule has an N–N triple bond, that is, one σ and a degenerate π bond, which is the standard bonding model for dinitrogen. The σ bond comes according to standard textbook explanations from the overlap of two sp-hybridized nitrogen AOs, which is suggested to be stronger than sp^2 or sp^3 bonds. However, a previous quantum chemical analysis by Kutzelnigg[25] concluded that the σ bond in N_2 is very weak or may even be repulsive. This is surprising considering the short bond and the high bond dissociation energy of N_2. The EDA data in Table 1 show that N_2 has very strong Pauli repulsion. The ΔE_{Pauli} value of 802.37 kcal mol^{-1} is the highest among the diatomic molecules investigated by us. The Pauli repulsion has an even higher absolute value than the ΔE_{orb} term, which means that the quantum theoretical terms $\Delta E_{orb}+\Delta E_{Pauli}$ yield net repulsion. The total interactions become strongly attractive because the quasiclassical interactions in N_2 significantly contribute to stabilization of the molecule ($\Delta E_{elstat}=-312.85$ kcal mol^{-1}). This comes from the overlap of the electron density in the nitrogen p(σ) AO with the nucleus of the other nitrogen atom (Figure 4). If one conceptually distinguishes between quantum theoretical interactions ($\Delta E_{orb}+\Delta E_{Pauli}$) and quasiclassical interactions (ΔE_{elstat}), then it follows that dinitrogen is a stable molecule only because of the contribution of the latter term. The sum of the terms $\Delta E_{orb}+\Delta E_{Pauli}$, the strengths of which depend

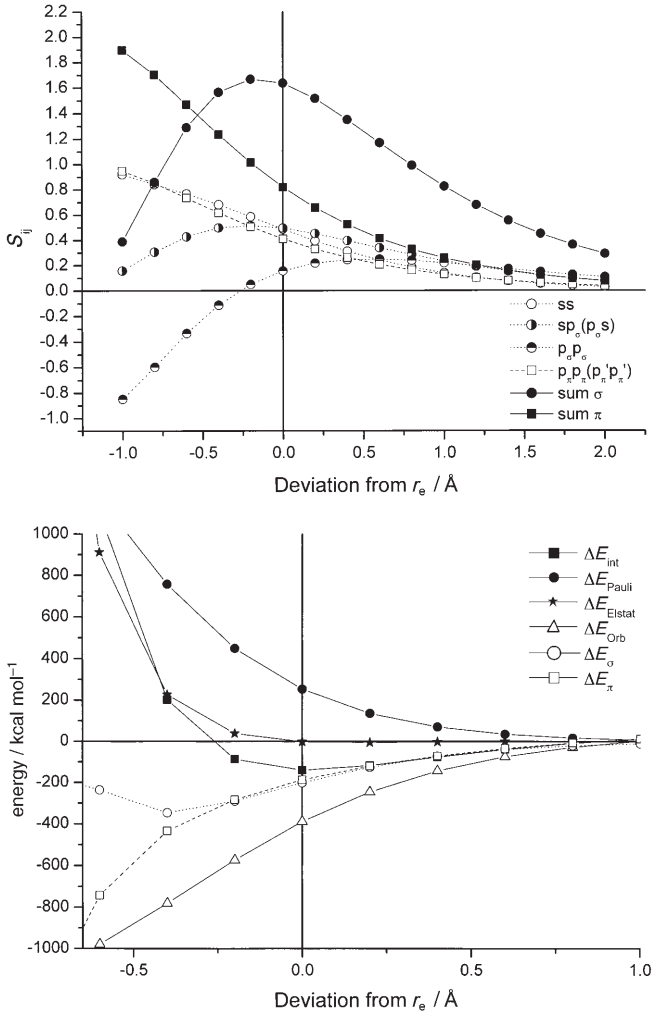

Figure 9. Top: Overlap integrals of the atomic 2s and 2p orbitals of C_2 as a function of the interatomic interaction. Bottom: Calculated EDA values for C_2 as a function of the interatomic distance. The reference value 0.0 is the calculated equilibrium bond length of 1.253 Å.

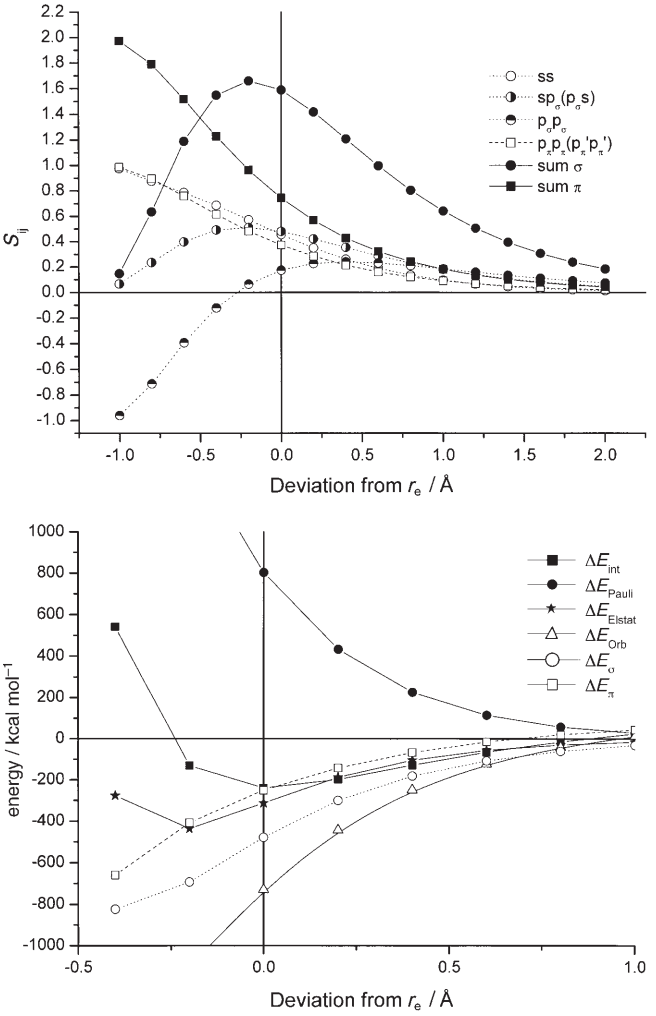

Figure 10. Top: Overlap integrals of the atomic 2s and 2p orbitals of N_2 as a function of the interatomic interaction. Bottom: Calculated EDA values for N_2 as a function of the interatomic distance. The reference value 0.0 is the calculated equilibrium bond length of 1.102 Å.

on the orbital overlap, yields net repulsion. The above partitioning is of course arbitrary, but the general statement about the triple bond in N_2 rests on an equally arbitrary partitioning which should be reconsidered in the light of the present results.

The EDA values in Table 1 support the conclusion of Kutzelnigg[25] that the σ bonding in N_2 may be repulsive. The total σ interactions ($\Delta E_{a1}+\Delta E_{Pauli}$) give a net contribution of $+323.56$ kcal mol^{-1}, while the π interactions are strongly attractive ($\Delta E(\pi)=-250.94$ kcal mol^{-1}), which is similar to the situation in C_2. A large difference between the two diatomics is the contribution of ΔE_{elstat} to the binding interactions, which is negligible for C_2 but very large for N_2, in which it is even larger than the BDE.

The trend of the orbital overlaps of N_2 (Figure 10 top) is similar to the data for C_2 and B_2, but the EDA curves of dinitrogen shown in Figure 10 (bottom) differ substantially from those of the lighter homologues. The curve for ΔE_{elstat} has a deep minimum of about -450 kcal mol^{-1} at a distance that is about 0.2 Å shorter than the equilibrium value for N_2. The strongly attractive interactions arising from the ΔE_{orb} and ΔE_{elstat} terms are annihilated by the very strong Pauli repulsion, which prevents the N–N distance attaining a value at which $S(\sigma)$ is a maximum.

The EDA results for O_2 (Table 1) indicate that all energy terms have smaller absolute values compared with N_2. This is reasonable because the interatomic distance of O_2 (1.224 Å) is longer than the N_2 equilibrium bond length (1.102 Å). Figure 4 shows that O_2 is the first molecule in the series in which there is Pauli repulsion between π electrons, because the oxygen atoms have a doubly occupied p(π) AO interacting with a singly occupied p(π) orbital of the other atom. The value $\Delta E_{Pauli}=464.93$ kcal mol^{-1} may thus not be considered anymore as part of the σ interactions, although the contribution of the π electrons to the Pauli repulsion will be much smaller than σ Pauli repulsion because the overlap of the former is clearly smaller than $S(\sigma)$ (see Figure 11). The quasiclassical electrostatic attraction

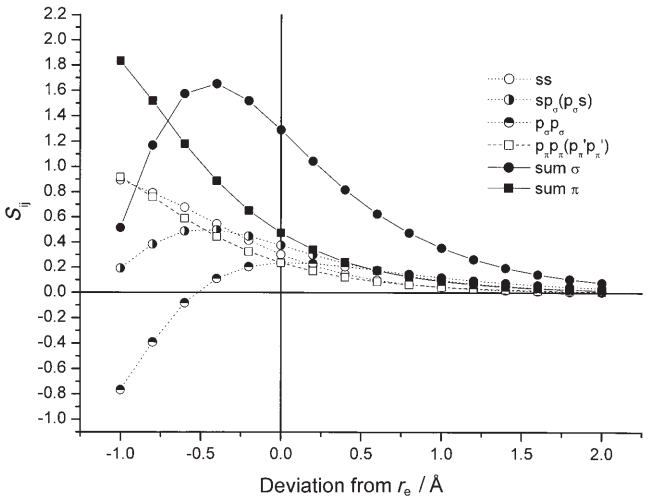

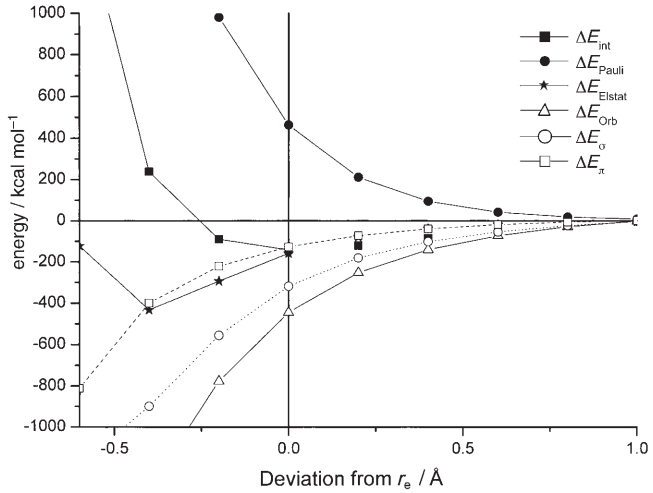

Figure 11. Top: Overlap integrals of the atomic 2s and 2p orbitals of O_2 as a function of the interatomic interaction. Bottom: Calculated EDA values for O_2 as a function of the interatomic distance. The reference value 0.0 is the calculated equilibrium bond length of 1.224 Å.

$\Delta E_{elstat} = -159.74$ kcal mol^{-1} is slightly stronger than the total interaction energy $\Delta E_{int} = -141.87$ kcal mol^{-1}. The quantum theoretical terms ΔE_{Pauli} ($+464.93$ kcal mol^{-1}) and ΔE_{orb} (-447.07 kcal mol^{-1}) nearly cancel each other. From a conceptual point of view it can thus be stated that dioxygen is bonded because of quasiclassical attraction. Beyond conceptual biases, it can be concluded that, without the stabilizing contribution of ΔE_{elstat}, O_2 would not be a stable molecule.

As noted above, the two components of the π orbital interactions in the triplet state of O_2 have slightly different values. This is because a spin change of one electron in a p(π) orbital takes place during the EDA calculation, since a triplet molecule is constructed from two triplet fragments. Table 1 shows that the $\Delta E(\pi)$ contributions are $\Delta E_{b1} = -59.11$ kcal mol^{-1} and $\Delta E_{b2} = -68.48$ kcal mol^{-1}. Thus, π bonding is a significant component of the binding interactions in O_2, although it is weaker than in N_2 and C_2. Note, however, that a direct comparison of the $\Delta E(\pi)$ values in O_2 with the values for C_2 and N_2 does not give a valid estimate of the relative strength of π interactions, because the Pauli repulsion in O_2 has a π component that is absent in C_2 and N_2.

The curves for the orbital overlaps given in Figure 11 (top) show that the maximum of $S(\sigma)$ lies 0.4 Å below the equilibrium distance. The equilibrium distance of O_2 is shifted further away from the maximum of $S(\sigma)$ towards a longer bond compared with N_2, although dioxygen has a σ and a π bond. All attractive components of the interatomic interaction in O_2 become stronger when the bond gets shorter (Figure 11 bottom). To compare the strength of the energy components for the more strongly bonded diatomic molecules B_2–F_2 at the same interatomic distance, we carried out EDA calculations using the equilibrium bond length of N_2 ($r = 1.102$ Å). The results are shown in Table 3.

The EDA values for O_2 at $r = 1.102$ Å give the expected increase of the absolute values for all components of the energy partitioning at the shorter distance. Note that the Pauli repulsion for O_2 ($\Delta E_{Pauli} = 740.58$ kcal mol^{-1}) is less than that calculated for N_2 ($\Delta E_{Pauli} = 802.37$ kcal mol^{-1}). This is surprising at first sight, because there is additional Pauli repulsion of the π electrons in O_2. The weaker Pauli repulsion in dioxygen compared with dinitrogen can be explained by the more compact atomic orbitals of oxygen, which lead to a smaller overlap in O_2. In fact, the absolute values of *all* energy terms of O_2 remain smaller than those of N_2 at the equilibrium distance of the latter. The same reasoning in terms of more compact orbitals can also be employed to explain the smaller ΔE_{Pauli} value of C_2 (392.38 kcal mol^{-1}) compared with B_2 ($\Delta E_{Pauli} = 438.61$ kcal mol^{-1}) when $r = 1.102$ Å. At the shorter distance the π orbital interactions in C_2 (2×-128.45 kcal mol^{-1}) become slightly stronger than the π bonding in N_2 (2×-125.47 kcal mol^{-1}).

The EDA results for F_2 (Table 1) show a further decrease in the absolute values of the energy terms compared with

Table 3. Energy partitioning analysis of the strongly bonded first-row diatomics E_2 at the fixed distance r(E–E) = 1.102 Å at BP86/TZ2P. Energies in kcal mol^{-1}.

	B	C	N	O	F
El. state	$^3\Sigma_g^-$	$^1\Sigma_g^+$	$^1\Sigma_g^+$	$^3\Sigma_g^-$	$^1\Sigma_g^+$
ΔE_{int}	86.37	−113.08	−240.23	−125.75	28.61
ΔE_{Pauli}	438.61	392.38	802.37	740.58	616.62
ΔE_{elstat}[a]	−3.90 (1.1%)	+20.83	−312.85 (30.0%)	−235.98 (27.2%)	−154.65 (26.3%)
ΔE_{orb}[a]	−348.34 (98.9%)	−526.29	−729.76 (70.0%)	−630.34 (72.8%)	−433.37 (73.7%)
ΔE_{a1}[b] (σ)	−198.56 (57.0%)	−269.38 (51.2%)	−478.81 (65.6%)	−451.26 (71.6%)	−398.95 (92.1%)
ΔE_{a2}[b] (δ)	0.00	0.00	0.00	0.00	0.00
ΔE_{b1}[b] (π)	−74.89 (21.5%)	−128.45 (24.4%)	−125.47 (17.2%)	−94.36 (15.0%)	−17.21 (4.0%)
ΔE_{b2}[b] (π)	−74.89 (21.5%)	−128.45 (24.4%)	−125.47 (17.2%)	−84.72 (13.4%)	−17.21 (4.0%)

[a] Values in parentheses are percentage contributions to the total attractive interactions $\Delta E_{elstat} + \Delta E_{orb}$. [b] Values in parentheses are percentage contributions to the total orbital interactions ΔE_{orb}.

O_2. We note the very small contribution of the quasiclassical electrostatic attraction in difluorine ($\Delta E_{elstat} = -41.20$ kcal mol^{-1}). This value is only a little higher than in B_2 ($\Delta E_{elstat} = -33.14$ kcal mol^{-1}). The contribution of the σ orbital interactions ($\Delta E_{a1} = -151.49$ kcal mol^{-1}) just compensates for the Pauli repulsion ($\Delta E_{Pauli} = 146.07$ kcal mol^{-1}). The small stabilizing contribution from the π orbitals (6.26 kcal mol^{-1}), which comes from relaxation of the orbitals, is negligible.

The rather weak bond in F_2 is often explained in terms of unusually strong Pauli repulsion between the lone-pair (π) electrons. The EDA data calculated at the short distance of $r = 1.102$ Å (Table 3) do not support this explanation. The ΔE_{Pauli} value for F_2 (616.62 kcal mol^{-1}) is still smaller than for O_2 (740.58 kcal mol^{-1}) and even for N_2 (802.37 kcal mol^{-1}), although the number of electron pairs which have the same spin increases from nitrogen to fluorine. The calculated ΔE_{Pauli} values show that F_2 would benefit from 185.75 kcal mol^{-1} less Pauli repulsion than N_2 at the same interatomic distance of $r = 1.102$ Å. The reason for the weak F–F bond must come from poor attraction. One contributing factor is the loss of π bonding, which provides 256.90 kcal mol^{-1} to the bonding interactions in N_2 (Table 1). A second factor is the weaker σ bond in F_2. However, Table 3 shows that, at the same distance of $r = 1.102$ Å, the $\Delta E_{a1}(\sigma)$ value for F_2 (−398.95 kcal mol^{-1}) is only 79.86 kcal mol^{-1} less than for N_2 (−478.81 kcal mol^{-1}). The crucial factor which makes the chemical bonding in difluorine unusually weak is the poor electrostatic attraction. Table 2 shows that the ΔE_{elstat} value of F_2 (−154.65 kcal mol^{-1}) is 158.20 kcal mol^{-1} less than in N_2 (−312.85 kcal mol^{-1}). Without the dramatic loss of electrostatic attraction difluorine would have a normal bond strength, that is, F_2 would be more strongly bound than Cl_2. This has previously been shown in a comparative study of the chemical bond in dihalogens F_2–I_2 by EDA.[3a] The trends of ΔE_{Pauli} and ΔE_{orb} exhibit the expected behavior of increasing strength from I_2 to F_2. This is in contrast to the values for ΔE_{elstat}, which first increase from I_2 to Cl_2 but then decrease for F_2. The 2p orbitals are very compact because there is no lower lying atomic p shell.[31]

Figure 12 (top) shows that the maximum of $S(\sigma)$ for F_2 occurs at a much shorter distance than the equilibrium value. The difference between the calculated bond length and $r[S(\sigma) = \max]$ is greater than 0.7 Å. The attractive energy components of the F–F interactions increase when the bond gets shorter by up to about 0.6 Å, at which the electrostatic attraction has its largest value. The increase in Pauli repulsion prevents further bond shortening. As noted above, it is not ΔE_{Pauli} that exhibits unusual behavior. The attractive components in the bonding region are weaker than in O_2 and N_2.

The peculiar trend of the ΔE_{elstat} values for E_2 exhibited in Table 1 demands analysis in more detail. In particular, the weak electrostatic attraction in C_2 and F_2 will be addressed. To understand the trend on a more equal footing we first calculated the ΔE_{elstat} values and its components nuclear–nuclear repulsion ΔE_{elstat}(N–N), nuclear–electron attraction

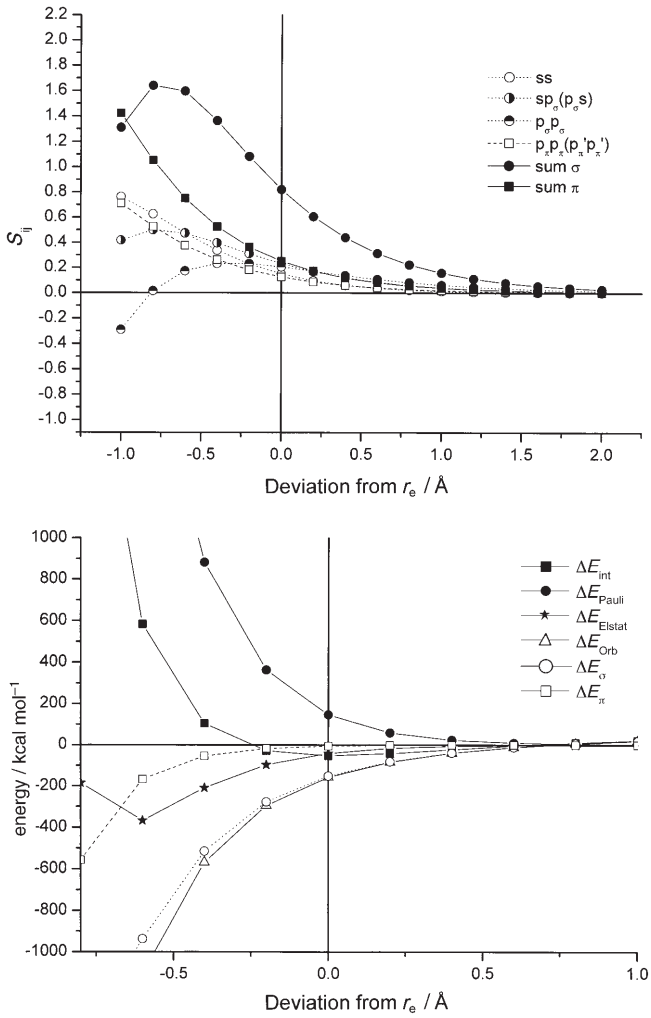

Figure 12. Top: Overlap integrals of the atomic 2s and 2p orbitals of F_2 as a function of the interatomic interaction. Bottom: Calculated EDA values for F_2 as a function of the interatomic distance. The reference value 0.0 is the calculated equilibrium bond length of 1.420 Å.

ΔE_{elstat}(N–e), and electron–electron repulsion ΔE_{elstat}(e–e) at the same distance. We chose the equilibrium bond length of diboron ($r = 1.617$ Å) for the comparison because it is intermediate between the shortest and the longest bond lengths, which occur in N_2 and Li_2, respectively. The results are given in Table 4.

The ΔE_{elstat} values shown in Table 4 increase toward attraction from Li_2 to Be_2, but then they decrease for B_2 and C_2. After this they increase again for N_2 before decreasing for O_2 and F_2. Since the interatomic distances are the same, the remaining variables that determine the electrostatic interactions are the nuclei and the size and shape [s, p(σ), p(π)] of the orbitals. We wanted to find out whether the trend of the ΔE_{elstat} values in Table 4 is determined more by the attractive interactions ΔE_{elstat}(N–e) or through alteration of the repulsive contributions ΔE_{elstat}(N–N) and ΔE_{elstat}(e–e). To this end we normalized the ΔE_{elstat}(N–e) values by dividing them by the number of electrons e_n and the nuclear charge $Z = N_m$. The calculated ΔE_{elstat}(N–e)/$e_n N_m$ in Table 4

Table 4. Partitioning of the ΔE_{elstat} term of E_2 at $r(E-E)=1.617$ Å into nuclear–nuclear repulsion $\Delta E_{elstat}(N-N)$, nuclear–electron attraction $\Delta E_{elstat}(N-e)$, and electron–electron attraction $\Delta E_{elstat}(e-e)$. Energies in kcal mol^{-1}.

	Li_2	Be_2	B_2	C_2	N_2	O_2	F_2
$\Delta E_{elstat}(N-N)$	1848.17	3285.64	5133.81	7392.69	10062.27	13142.56	16633.55
$\Delta E_{elstat}(N-e)$	−3440.24	−6361.20	−9915.54	−14331.76	−20034.72	−26096.42	−32998.84
$\Delta E_{elstat}(N-e)/e_nN_m$[a]	−191.13	−198.80	−198.30	−199.05	−204.44	−203.88	−203.70
$\Delta E_{elstat}(e-e)$	1594.08	3020.88	4748.59	6935.94	9898.58	12914.21	16348.24
$\Delta E_{elstat}(e-e)/e_l$[b]	177.12	188.81	189.94	192.67	202.01	201.78	201.83
ΔE_{elstat}	2.01	−54.68	−33.14	−3.13	−73.87	−39.65	−17.05

[a] Nuclear–electron attraction divided by the number of electrons e_n of E_2 and the nuclear charge N_m of E. [b] Electron–electron repulsion divided by the number of interatomic electron pairs e_l.

give the average nuclear–electron attraction between one electron and the nuclear charge $Z=+1$. We also normalized the $\Delta E_{elstat}(e-e)$ values by dividing them by the number of interacting electron pairs e_l. The $\Delta E_{elstat}(e-e)/e_l$ values are also shown in Table 4.

The calculated values for $\Delta E_{elstat}(N-e)/e_nN_m$ and $\Delta E_{elstat}(e-e)/e_l$ are compared with the values for interacting point charges given by Coulomb's law at $r=1.617$ Å (± 205.35 kcal mol^{-1}). Table 4 shows that the largest deviation from the point-charge value is calculated for Li_2. This is reasonable because Li has the most diffuse valence orbital of the second-row elements. However, the weakening of the e–e repulsion at $r=1.617$ Å is not large enough to compensate for the weaker N–e attraction, which yields weak overall repulsion.[29] The smallest deviation from the point-charge value is calculated for N_2. The elements oxygen and fluorine are more electronegative than nitrogen and their orbitals are therefore tighter than those of nitrogen. However, the atomic orbitals which are filled when one goes from N_2 to O_2 and F_2 are p(π) AOs, which clearly exhibit larger deviation from the point-charge model (see Figure 3 (left) and discussion above).

The calculated data show that the increase in total electrostatic attraction from Li_2 to Be_2 comes from the larger attractive term $\Delta E_{elstat}(N-e)/e_nN_m$, which increases from −191.13 kcal mol^{-1} for one electron for Li_2 to −198.80 kcal mol^{-1} for Be_2. The difference is 7.67 kcal mol^{-1}. Diberyllium has eight electrons that give a total contribution of 8×-7.67 kcal mol^{-1} $=-61.36$ kcal mol^{-1} from stronger nuclear–electron attraction. This is even a little higher than the increase in ΔE_{elstat} from +2.01 kcal mol^{-1} to −54.68 kcal mol^{-1}.

In contrast to the change from Li_2 to Be_2, the decrease in ΔE_{elstat} from Be_2 to B_2 and C_2 does not come from weaker N–e attraction, but mainly from stronger E–e and N–n repulsion. Table 4 shows that the $\Delta E_{elstat}(N-e)/e_nN_m$ value of B_2 (−198.30 kcal mol^{-1}) is a little smaller, while that of C_2 (−199.05 kcal mol^{-1}) is a little larger than that of Be_2. The decrease in the $\Delta E_{elstat}(N-e)/e_nN_m$ value of B_2 by 0.50 kcal mol^{-1} yields $10\times 0.50=5.0$ kcal mol^{-1} less electrostatic attraction, but ΔE_{elstat} decreases from −54.68 kcal mol^{-1} to −33.14 kcal mol^{-1}, which gives a reduction by 21.54 kcal mol^{-1}. The change from B_2 to C_2 is accompanied by further weakening of ΔE_{elstat} from −33.14 kcal mol^{-1} to −3.13 kcal mol^{-1}, which gives a difference of 30.01 kcal mol^{-1}. But the $\Delta E_{elstat}(N-e)/e_nN_m$ value *increases* from B_2 to C_2. It follows that the weaker electrostatic attractions in B_2 and C_2 come from stronger electron–electron and nuclear–nuclear repulsion.

The above quantitative results can be qualitatively understood when the shapes of the orbitals are considered. From Li_2 to Be_2 the 2s AOs of the atoms become doubly filled to give σ bonds that accumulate electronic charge between the nuclei, which have a higher positive charge in Be than in Li.[30] This enhances the nuclear–electron attraction. But from Be_2 to B_2 and C_2 the additional electrons occupy the p(π) AOs (Figure 4), which are oriented perpendicular to the bond. Table 4 shows that the average nuclear–electron attraction remains nearly the same but the average repulsion becomes larger. It can be explained by the nuclei being less effectively shielded by the π electrons. This is shown in Figure 3 (right). The net electrostatic interaction of the electrons occupying the 2p(π) AOs is repulsive.

The same trend is observed from C_2 to N_2, O_2, and F_2. Two more electrons occupying the p(σ) AOs in N_2 (Figure 4) enhance the nuclear–electron attraction. Table 4 shows that the $\Delta E_{elstat}(N-e)/e_nN_m$ value increases from C_2 (−199.05 kcal mol^{-1}) to N_2 (−204.44 kcal mol^{-1}) by 5.39 kcal mol^{-1} for one electron. N_2 has 14 electrons. The increase of 14×-5.39 kcal mol^{-1} $=-75.40$ kcal mol^{-1} matches the total increase of ΔE_{elstat} from −3.13 kcal mol^{-1} in C_2 to −73.87 kcal mol^{-1} in N_2. The next electrons occupy p(π) orbitals in O_2 and F_2. Table 4 shows that the $\Delta E_{elstat}(N-e)/e_nN_m$ values for O_2 (−203.88 kcal mol^{-1}) and F_2 (−203.70 kcal mol^{-1}) change very little, while ΔE_{elstat} in F_2 (−17.05 kcal mol^{-1}) and O_2 (−39.65 kcal mol^{-1}) is clearly weaker than in N_2 (−73.87 kcal mol^{-1}). We conclude that the stronger electrostatic attraction in N_2 comes from enhanced nuclear–electron attraction, while the weaker electrostatic attraction in O_2 and F_2 comes from larger nucleus–nucleus and electron–electron repulsion.

The trend of the ΔE_{elstat} values in Table 4 agrees with the above conclusion that electrons in more compact orbitals behave more like point charges, which means less net attraction, but the shapes of the AOs need to be considered. The orbitals become more compact from left to right in a row of the periodic table. The increase of ΔE_{elstat} from C_2 to N_2 is due to occupation of the p(σ) AOs in dinitrogen. The exception to the trend is the increase of ΔE_{elstat} from Li_2 to Be_2, which cannot be explained by the shape of the orbitals. Li_2 should have a much stronger bond because of its diffuse 2s

orbital. Kutzelnigg pointed out that the bond in Li_2 is unusual because the orbital is so diffuse.[25] Another factor which may play a role in the weak Li–Li bond is that the nucleus of Li is rather small. To elucidate the roles of the orbital and the size of the nucleus in the electrostatic attraction, we calculated Li_2 and Be_2 using orbitals for which the exponents were exchanged, that is, Li_2 has the atomic orbitals of Be, while Be_2 has the atomic orbitals of Li. The EDA calculations show that ΔE_{elstat} of Li_2 decreases from −8.30 to −2.64 kcal mol^{-1} when the Be orbitals are used, while the electrostatic attraction in Be_2 increases from −17.87 to −35.90 kcal mol^{-1} when the Li orbitals are employed. This is striking evidence that the rather weak electrostatic attraction in Li_2 comes from the less positively charged atomic nucleus of Li.

We analyzed the electrostatic interactions in the strongly bonded diatomic molecules B_2–F_2 in more detail by partitioning the N–e and e–e terms into contributions from electrons in orbitals having different symmetry. The data are shown in Table 5. The decomposition of the electrostatic terms of ΔE_{elstat}(N–e) and ΔE_{elstat}(e–e) into contributions from electrons in orbitals with different symmetry was achieved by calculating the electrostatic interactions between positively charged atoms in E_2^{q+} ($q = 2$–6) with electrons removed from specific atomic orbitals. The frozen orbitals of E_2 were used to describe the MOs in E_2^{q+}, and this guarantees that the ΔE_{elstat} values of the occupied orbitals remain the same as in the neutral molecule. The calculated values and the formulas which were used to determine the energy values are given in the Supporting Information.

The data in Table 5 show that the largest contributions to the N–e attraction and the e–e repulsion come from the electrons in the s orbitals that are fully occupied in the molecules. More interesting information comes from the electrostatic interactions of a single electron which occupies an s, p(σ), or p(π) AO. Table 5 shows the sum of the N–e and e–e interactions for single electrons in orbitals with different symmetry. The data $[\Delta E_{elstat}(N–e) + \Delta E_{elstat}(e–e)]/e$ give a quantitative measure for the deviation of the electrostatic interaction of an electron in the molecule from the value that is predicted by Coulomb's law for point charges. The latter value is given by the calculated nuclear–nuclear repulsion per proton $\Delta E_{elstat}(N–N)/p$. The data show that the electrons in the s and particularly in the p(σ) AOs contribute to the quasiclassical electrostatic attraction, while the electrons in the p(π) AO have a repulsive contribution because they do not compensate for the n–n repulsion. In other words, the shielding of the nuclear–nuclear repulsion by the electrons has the order p(σ) > s > p(π). It also becomes evident from the values in Table 5 why the electrostatic attraction in F_2 is so small. The ΔE_{elstat} values for a single electron are much closer to the ΔE_{elstat} value for a proton than in the other diatomic molecules. The electrons in F_2 are in much more compact orbitals than in the lighter analogues and their electrostatic interactions approach point-charge values.

We addressed the question to what extent the strong electrostatic attraction in the diatomic molecules may change after Pauli repulsion and orbital interactions polarize the electronic charge of the atoms. The electron density distribution in the atomic basin in a molecule is not the same as

Table 5. Partitioning of ΔE_{elstat} into contributions from nuclear–-nuclear repulsion ΔE_{elstat}(N–N) and from electrons in different orbitals to nuclear–electron attraction ΔE_{elstat}(N–e) and electron-electron repulsion ΔE_{elstat}(e–e) calculated at the equilibrium bond lengths. Energies in kcal mol^{-1}.

		Li_2	Be_2	B_2	C_2	N_2	O_2	F_2
ΔE_{elstat}(N–N)		1094.14	2175.74	5133.81	9538.04	14771.35	17359.66	18936.27
ΔE_{elstat}(N–e)[a]								
	$[1s^2 2s^2]$	−2158.90 (6)	−4331.20 (8)	−8141.54 (8)	−12581.84 (8)	−16726.48 (8)	−17331.70 (8)	−16843.66 (8)
	2p(σ)	–	–	–	–	−4686.42 (2)	−4795.04 (2)	−4532.72 (2)
	2p(π)	–	–	−1774.00 (2)	−5493.28 (4)	−7410.32 (4)	−12019.96 (6)	−16079.68 (8)
ΔE_{elstat}(e–e)[b]								
	2p(π)–2p(π)	–	–	156.03 (1)	831.01 (4)	968.86 (4)	2121.19 (9)	3442.11 (16)
	2p(σ)–2p(σ)	–	–	–	–	308.08 (1)	301.42 (1)	264.09 (1)
	2p(π)–2p(σ)	–	–	–	–	1090.52 (4)	1586.23 (6)	1886.07 (8)
	2p(π)–$[1s^2 2s^2]$	–	–	1403.84 (8)	3609.96 (16)	4182.32 (16)	5986.38 (24)	7145.78 (32)
	2p(σ)–$[1s^2 2s^2]$	–	–	–	–	2509.18 (8)	2328.26 (8)	1999.30 (8)
	$[1s^2 2s^2]$–$[1s^2 2s^2]$	1056.46 (16)	2137.59 (16)	3188.72 (16)	4092.89 (16)	4680.06 (16)	4303.82 (16)	3741.22 (16)
$\Delta E_{elstat}(N–e) + \Delta E_{elstat}(e–e)/e$[c]								
	$[1s^2 2s^2]$	−183.74	−274.20	−531.36	−835.50	−1087.58	−1108.82	−1066.24
	ΔE $[1s^2 2s^2]$[d]	−1.38	−2.23	−17.98	−40.66	−32.48	−23.84	−14.22
	2p(σ)	–	–	–	–	−1289.25	−1268.19	−1162.97
	ΔE [2p(σ)][d]	–	–	–	–	−234.15	−183.21	−110.95
	2p(π)	–	–	−458.03	−714.32	−951.26	−1018.68	−1015.21
	ΔE [2p(π)][d]	–	–	55.35	80.52	103.84	66.30	36.81
$\Delta E_{elstat}(N–N)/p$[e]		182.36	271.97	513.38	794.84	1055.10	1084.98	1052.02
ΔE_{elstat}		−8.30	−17.87	−33.14	−3.22	−312.85	−159.74	−41.20

[a] The data in parentheses are the numbers of interacting electrons in the electron–nuclear attraction. [b] The data in parentheses are the numbers of interacting electron pairs in the electron–electron repulsion. [c] Sum of electron–nuclear attraction and electron–electron repulsion per electron. [d] Difference between ΔE_{elstat} per electron and ΔE_{elstat} per proton. [e] Nuclear–nuclear repulsion per proton.

in the free atom. If the electrostatic interactions in the molecule were correctly described by Coulomb's law, the attractive forces would even become *higher* than in the EDA calculations which are discussed in this paper. This is because the polarization lowers the total energy of the molecule. However, quantum theoretical interactions could in principle weaken the interatomic quasiclassical attraction, because the Pauli repulsion removes charge from the interatomic region. We therefore analyzed the changes in the electron density in N_2 that occur in steps 2 and 3 of the EDA calculations after superimposing the electron densities of the fragments, that is, when the wavefunction first becomes subject to antisymmetrization and renormalization and then relaxes through orbital interactions. We chose N_2 because it has the largest ΔE_{elstat} value of the calculated molecules. The changes in electron density are shown in Figure 13.

Figure 13 (top) illustrates that antisymmetrization and renormalization in the ΔE_{Pauli} step lead to removal of electronic charge from the nitrogen–nitrogen bonding region but the following relaxation in the ΔE_{orb} step (Figure 13 middle) restores electron density in the area of σ and π bonding. Clearly, the interatomic electronic charge which is withdrawn in the ΔE_{Pauli} step becomes accumulated in the backside σ regions of the atoms. In the ΔE_{orb} step electronic charge is transferred from the atomic p(π) region to the interatomic area of σ and π bonding, but the charge concentration in the backside σ regions is also further enhanced. Figure 13 (bottom) shows the total changes which occur in the previous two steps. The quantum theoretically induced changes in the electron density lead to stronger accumulation along the internuclear axis in the σ- and π-bonding interatomic region and in the backside area, while electronic charge is removed from the p(π) area of the atoms. This should further enhance the attractive contribution of the electrons in s and p(σ) orbitals to the ΔE_{elstat} term. From this it can be concluded that the quasiclassical electrostatic bonding with the polarized atomic charges should be even stronger than with the unpolarized charges employed in the EDA.

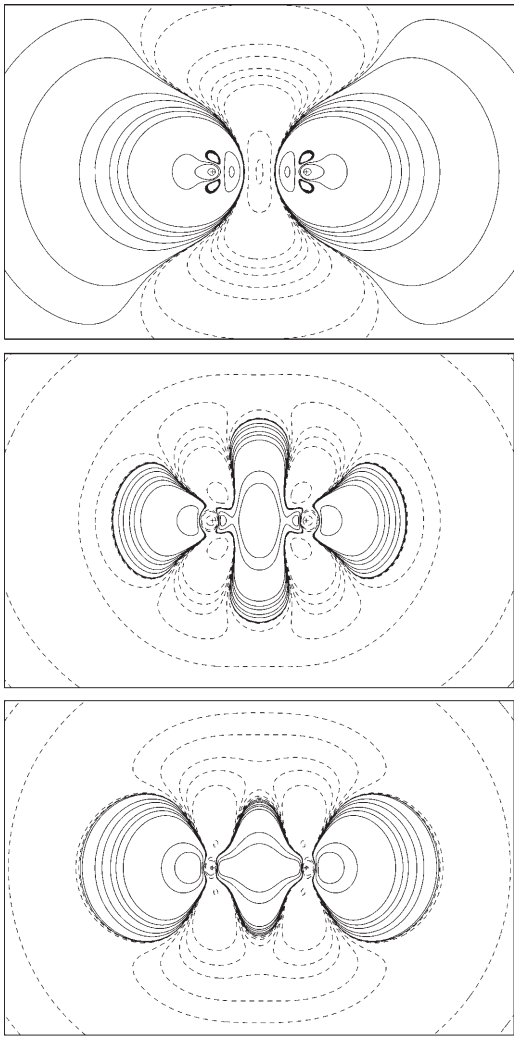

Figure 13. Changes in the electron density of N_2 during the EDA. Solid lines indicate charge accumulation, and dashed lines charge depletion. Top: Antisymmetrization and renormalization. Middle: Orbital relaxation. Bottom: Total changes during top and middle steps.

In summary, the trend of the ΔE_{elstat} values shown in Table 1 can be understood in terms of the shape and the size of the atomic orbitals of E_2. The deviation of the data calculated with the quasiclassical approximation from the point-charge model explains why the contribution of the electrostatic attraction to the bond energy can be very large even in nonpolar molecules. The quasiclassical attraction is particularly strong when the electron occupies a p(σ) AO.

Diatomic molecules Na_2–Cl_2: Judgment based on experience teaches that the chemical behavior of main group elements of the third and higher rows of the periodic system is significantly different from the chemistry of the second-row atoms Li–F. According to Kutzelnigg, much of the difference comes from the fact that the latter elements have 2p valence orbitals that penetrate rather deeply into the 1s core because there is no lower lying shell of filled p orbitals.[31] The radius of the 2s and 2p AOs is very similar, and thus the 2s and 2p orbitals overlap quite well, and this leads to efficient sp^x hybridization. The different spatial extension of the higher order (*n*)s and (*n*)p orbitals makes their hybridization less efficient, although their energy difference is less than that between the 2s and 2p orbitals. Kutzelnigg also showed that the lower chemical stability of multiple bonds between heavier main-group elements is not caused by a smaller overlap of the p(π) AOs, as is often assumed.[31]

We wanted to know whether an energy partitioning analysis gives significantly different results for the bonding in heavier main-group compounds compared with the lighter homologues. In the following we discuss the results of the EDA calculations for the third-row diatomic molecules E_2 (E = Na–Cl). Table 6 gives the EDA results at the equilibrium distances. The calculated overlap integrals and the EDA results for Al_2, P_2, and Cl_2 at different interatomic distances are given in Figures 14–16. The figures for the remaining compounds Na_2, Mg_2, Si_2, and S_2 are presented as Supporting Information.

Table 6. Energy partitioning analysis of the second-row dimers E_2 (E = Na–Cl) in C_{2v} at BP86/TZ2P (ZORA); the fragments were calculated in D_{2h}; all energies in kcal mol^{-1}, distances r(E–E) in Å, all dissociation energies were calculated for dissociation into the ground-state atoms (Na: ^{2}S; Mg: ^{1}S; Al: ^{2}P; Si: ^{3}P; P: ^{4}S; S: ^{3}P ; Cl: ^{2}P).

	Na	Mg	Al	Si	Si	P	S	Cl
State	$^1\Sigma_g^+$	$^1\Sigma_g^+$	$^3\Sigma_g^-$	$^3\Sigma_g^-$	$^1\Sigma_g^+$	$^1\Sigma_g^+$	$^3\Sigma_g^-$	$^1\Sigma_g^+$
ΔE_{int}	−16.25	−1.74	−35.55	−78.34	−56.48	−118.50	−112.20	−64.60
ΔE_{Pauli}	5.07	9.39	42.93	184.24	79.47	317.43	247.32	129.11
ΔE_{elstat}[a]	−10.67	−5.15	−15.62	−123.73	−4.39	−186.25	−121.80	−51.05
	(50.1 %)	(46.2 %)	(19.9 %)	(47.1 %)	(3.2 %)	(42.7 %)	(33.9 %)	(26.4 %)
ΔE_{orb}[b]	−10.65	−5.99	−62.87	−138.85	−131.56	−249.68	−237.73	−142.66
	(49.9 %)	(53.8 %)	(80.1 %)	(52.9 %)	(96.8 %)	(57.3 %)	(66.1 %)	(73.6 %)
ΔE_{a1} (σ)	−10.66	−5.99	−26.11	−91.70	−50.12	−148.63	−153.97	−126.72
	(100.0 %)	(100.0 %)	(41.5 %)	(66.0 %)	(38.1 %)	(59.5 %)	(64.8 %)	(88.8 %)
ΔE_{a2} (δ)	0.0	0.0	0.0	0.0	0.0	0.0	0.0	0.0
ΔE_{b1} (π)	0.0	0.0	−18.38	−26.16	−40.72	−50.52	−44.73	−7.97
	(<0.1 %)	(<0.1 %)	(29.2 %)	(18.9 %)	(31.0 %)	(20.2 %)	(18.8 %)	(5.6 %)
ΔE_{b2} (π)	0.0	0.0	−18.38	−20.99	−40.72	−50.52	−39.03	−7.97
	(<0.1 %)	(<0.1 %)	(29.2 %)	(15.1 %)	(31.0 %)	(20.2 %)	(16.4 %)	(5.6 %)
ΔE_{corr}[d]	0.25	0.00	1.07	1.73	1.64	1.28	2.97	2.60
D_e[c]	16.00	1.74	34.48	76.61	54.84	117.22	109.23	62.00
	(17.06)	(1.23)	(35.09)	(74.75)		(117.18)	(101.80)	(57.98)
r(E–E)[c]	3.095	3.607	2.510	2.303	2.071	1.911	1.921	2.023
	(3.0788(7))	(3.890(5))	(2.466)	(2.246)		(1.8934)	(1.8892)	(1.987(9))

[a] Values in parentheses are percentage contributions to the total attractive interactions $\Delta E_{elstat} + \Delta E_{orb}$. [b] Values in parentheses are percentage contributions to the total orbital interactions ΔE_{orb}. [c] Experimental values in parentheses from ref. [11a]. [d] Correction for spin polarization.

The data in Table 6 show that the calculated bond lengths and bond energies are in reasonable agreement with experiment. All diatomic molecules of the third row Na_2–Cl_2 have weaker bonds than the second-row compounds Li_2–F_2, except for Cl_2, which is more strongly bonded than F_2. This will be discussed below. Another trend that holds for all compounds concerns the relative strength of the electrostatic interactions in E_2. Table 6 shows that the heavier diatomics Na_2–Cl_2 have a bigger percentage contribution of ΔE_{elstat} to the attractive interactions than the corresponding species Li_2–F_2.

Na_2 has equally strong contributions from attractive orbital interactions and electrostatic bonding, which are weakened by the Pauli repulsion. The ΔE_{Pauli} value is clearly larger (5.07 kcal mol^{-1}) than in Li_2 (1.76 kcal mol^{-1}) because the filled 2s core orbital of Na is bigger than the 1s core AO of Li. Unlike in Li_2, in which the chemical bonding is influenced by substantial polarization of the diffuse 2s AO, the 3s AO of Na appears to be relatively little polarized by bond formation in Na_2. Table 2 shows that the EDA calculation on Na_2 in which the polarization functions are deleted give a value for ΔE_{orb} (−9.58 kcal mol^{-1}) which is only slightly smaller than that calculated with the full basis set (−10.67 kcal mol^{-1}). The weaker 3s/3p hybridization in Na_2 compared with the 2s/2p hybridization in Li_2 is in agreement with the statement of Kutzelnigg[31] that sp^x hybridization in heavier elements is less efficient than in atoms of the first octal row. The very weak bond in Mg_2 (Table 6), which hardly qualifies as a true chemical bond, comes from weak interactions which we do not further analyze here.

The quantum chemical σ interactions in Al_2 ($\Delta E_{a1} + \Delta E_{Pauli}$) are repulsive. The chemical bonding comes from the π orbital interactions and the quasiclassical electrostatic attraction yielding an Al–Al bond, which is half as strong as the B–B bond (Table 6), but the nature of the two bonds is otherwise very similar. This comes even more evident when the curves for the overlap integrals and the EDA data at different interatomic distances are compared. The maximum of the σ overlap $S(\sigma)$ for Al_2 is shifted even more towards a shorter bond (Figure 14 top), but the shapes of the curves resemble very much those of B_2 (Figure 7 top). The conclusion also holds true for the curves of the EDA data (Figure 14 bottom). The increase in ΔE_{Pauli} prevents further shortening of the Al–Al bond, although the attractive contributions further increase up to about 1 Å below the equilibrium bond length. The chemical bond in Al_2 thus comes from nearly equally strong contributions of quasiclassical electrostatic attraction and genuine orbital interactions.

The electronic ground state of Si_2 is a triplet ($X^3\Sigma_g^-$) state in which the $3\sigma_g^+$ orbital (Figure 5) is doubly occupied, while the higher lying degenerate $1\pi_u$ MO is filled with two electrons having the same spin. The electronic valence configuration of Si_2 is thus different from that of C_2, which has a singlet ($X^1\Sigma_g^+$) ground state in which the $3\sigma_g^+$ orbital is above the $1\pi_u$ MO. The $^1\Sigma_g^+$ state with the valence configuration $(2\sigma_g)^2(2\sigma_u)^2(1\pi)^4$ is an excited state of Si_2, which was found experimentally to be 26.57 ± 0.23 kcal mol^{-1} higher in energy than the $X^3\Sigma_g^-$ state.[32] The BP86/TZ2P calculated value for the $X^3\Sigma_g^- \rightarrow {}^1\Sigma_g^+$ excitation energy of 21.77 kcal mol^{-1} is in reasonable agreement with experiment. In the EDA calculation on the interacting atoms in the $X^3\Sigma_g^-$ state, the two Si atoms were in the ^{3}P ground state. This is schematically shown in Figure 4. We analyzed Si_2 in both the $X^3\Sigma_g^-$ ground and $^1\Sigma_g^+$ excited electronic states.

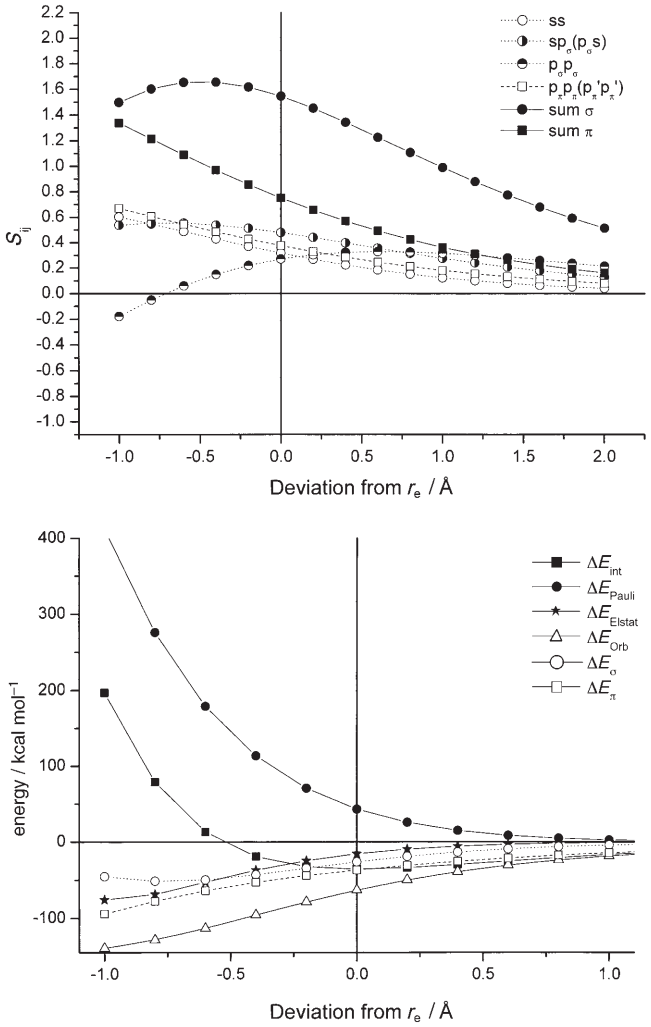

Figure 14. Top: Overlap integrals of the atomic 3s and 3p orbitals of Al_2 as a function of the interatomic interaction. Bottom: Calculated EDA values for Al_2 as a function of the interatomic distance. The reference value 0.0 is the calculated equilibrium bond length of 2.510 Å.

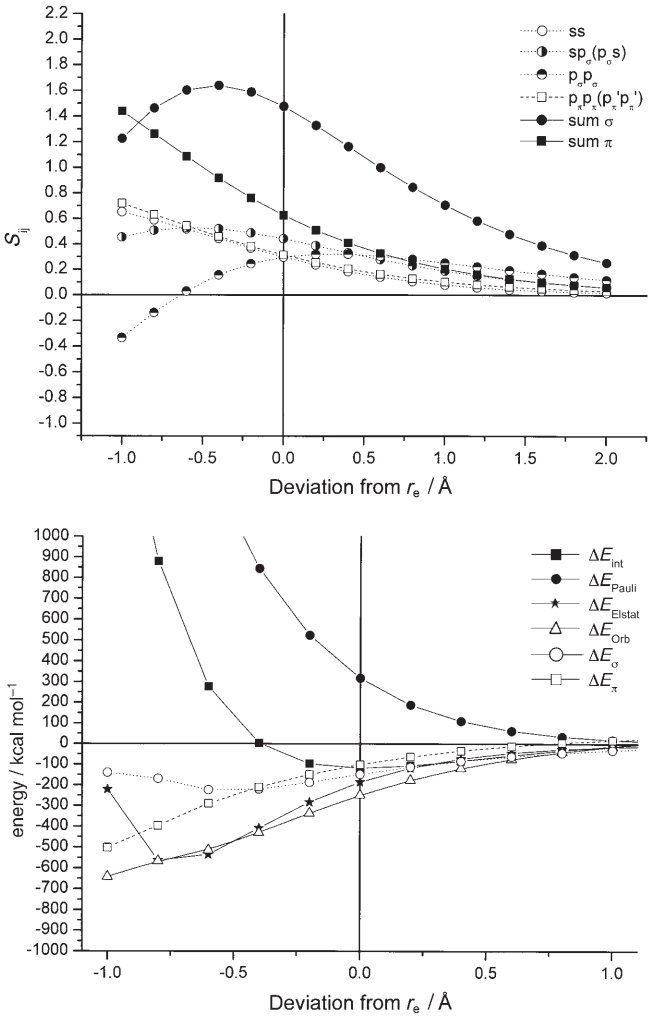

Figure 15. Top: Overlap integrals of the atomic 3s and 3p orbitals of P_2 as a function of the interatomic interaction. Bottom: Calculated EDA values for P_2 as a function of the interatomic distance. The reference value 0.0 is the calculated equilibrium bond length of 1.911 Å.

Table 6 shows that the binding interactions in the $^1\Sigma_g^+$ state of Si_2 have a negligible contribution from the quasiclassical electrostatic interactions. The ΔE_{elstat} value is only -4.39 kcal mol^{-1}. The attractive interactions come essentially from ΔE_{orb}, which contributes -131.56 kcal mol^{-1} to the bond energy. The σ component of the orbital interactions (-50.12 kcal mol^{-1}) is compensated by the Pauli repulsion (79.47 kcal mol^{-1}). From this it follows that Si_2 in its $^1\Sigma_g^+$ state is a π-bonded molecule like C_2, for which this is the ground state. The nature of the Si–Si bond in the $X^3\Sigma_g^-$ state is quite different from that in the $^1\Sigma_g^+$ state. Table 6 shows that the electrostatic term now becomes very large ($\Delta E_{elstat} = -123.73$ kcal mol^{-1}). This is reasonable because the p(σ) AOs of the atoms are occupied in the $X^3\Sigma_g^-$ state, but are empty in the $^1\Sigma_g^+$ state. This yields significantly stronger σ orbital interactions for the triplet state (-91.70 kcal mol^{-1}), although the bond is clearly longer (2.303 Å) than in the singlet state (2.071 Å). The π bonding in the triplet state is weaker than in the singlet state because of the longer bond. Note that the two π components in the $X^3\Sigma_g^-$ ground state of Si_2 are slightly different, as they are in the $X^3\Sigma_g^-$ ground state of O_2, because in the EDA calculation the spin of one p(π) electron changes. The Pauli repulsion in the triplet state of Si_2 (184.24 kcal mol^{-1}) is stronger than the total orbital interactions (-138.85 kcal mol^{-1}). Thus, the quantum chemical forces in the $X^3\Sigma_g^-$ state of Si_2 at the equilibrium geometry are repulsive, and the bonding now comes from ΔE_{elstat}.

The EDA results for P_2 (Table 6) show that the nature of the bonding is very similar to that in N_2 (Table 1). The sum of the quantum chemical terms $\Delta E_{orb} + \Delta E_{Pauli}$ gives a repulsive contribution to the interatomic interactions, while the attraction due to the electrostatic term ΔE_{elstat} is stronger than the BDE. It follows that P_2, like N_2, would not be a stable molecule without quasiclassical interactions. The orbital interactions in P_2 have slightly more π character (40.4%) than in N_2 (34.4%), but the former value probably includes a stronger contribution from polarization than the latter.

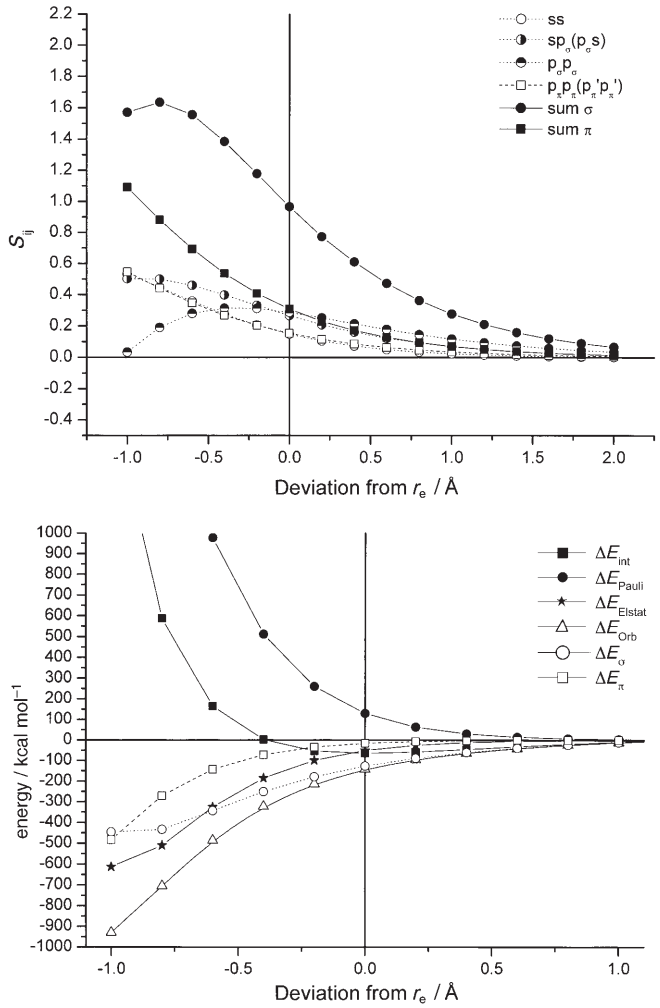

Figure 16. Top: Overlap integrals of the atomic 3s and 3p orbitals of Cl_2 as a function of the interatomic interaction. Bottom: Calculated EDA values for Cl_2 as a function of the interatomic distance. The reference value 0.0 is the calculated equilibrium bond length of 2.023 Å.

This becomes evident from the π-orbital contribution in the dihalogens, which arises only through polarization. The relative contribution of the $\Delta E_{orb}(\pi)$ value in Cl_2 (11.2%) is clearly larger than in F_2 (4.0%). The curves for the orbital overlaps and the EDA data for P_2 (Figure 15) have a similar shape to the curves for N_2 (Figure 9).

Great similarities in the nature of the bonding are also found between S_2 and O_2 and between Cl_2 and F_2 (Tables 1 and 5). Interestingly, the Pauli repulsions in S_2 and O_2 are slightly stronger than the attractive orbital interactions. The quasiclassical binding interactions ΔE_{elstat} are thus responsible in both species for the total bond energy. The ΔE_{orb} terms of Cl_2 and F_2 have slightly larger absolute values than the ΔE_{Pauli} term, but the net binding which comes from the quantum chemical terms is clearly less than the contribution of ΔE_{elstat}. Figure 16 shows that the curves for the orbital overlaps and the EDA data of Cl_2 closely resemble those for F_2 (Figure 11). It is tempting to cite the larger Pauli repulsion in F_2 compared to that in Cl_2 as the reason for the smaller bond energy of the former. That this hasty conclusion is not valid becomes evident when the EDA data for all dihalogens F_2–I_2 are compared. It was shown that the Pauli repulsion smoothly increases with the trend $I_2 < Br_2 < Cl_2 < F_2$, for which the last increase from Cl_2 to F_2 is less steep than the previous steps.[3a] The attractive orbital term also increases from I_2 to F_2. The quasiclassical electrostatic attraction ΔE_{elstat} first increases with $I_2 < Br_2 < Cl_2$, but then decreases again with $Cl_2 > F_2$. Thus, the trends of ΔE_{orb} and ΔE_{Pauli} exhibit regular behavior, while ΔE_{elstat} abnormally becomes smaller from Cl_2 to F_2. This is because the highly electronegative fluorine has very compact orbitals that lower the net electrostatic attraction between neutral atoms. Note that the ΔE_{elstat} values increase from S_2 to O_2 and from P_2 to N_2, while they decrease from Cl_2 to F_2. As noted above, the abnormally weak bond of F_2 is caused by an unusually small contribution of quasiclassical electrostatic bonding.

Table 7 classifies the chemical bonds in Li_2–F_2 and Na_2–Cl_2 in their electronic ground state according to the EDA calculations. The quasiclassical attraction plays an important or even dominant role for the interatomic attraction in nearly all diatomic molecules that we have investigated. To avoid misunderstanding, we emphasize that the classification does not mean that orbital interactions in molecules like N_2 and O_2 are unimportant. The chemical reactivity of both diatomic species can convincingly be discussed in terms of orbital interactions, particularly of the frontier orbitals. Chemical reactions are driven by energy changes which are small compared to the total energy of a molecule. The success of molecular orbital theory in explaining geometries and reactivities rests on the observation that energy differences associated with chemical processes correlate in many cases very well with orbital interactions.[33] This has led to the situation that chemical observations are now often discussed only in terms of orbital interactions, while other terms are neglected. Chemical bonding in covalent bonds is then thought to be only the result of ΔE_{orb}. The present work demonstrates that Pauli repulsion and quasiclassical electrostatic attraction are equally important for understanding chemical bonds. This holds true not only for the classification of the chemical bonds, it may also be important for understanding trends in interatomic interactions. As shown above, the

Table 7. Classification of the chemical bonds in diatomic molecules Li_2–F_2 and Na_2–Cl_2 in their electronic ground state in terms of quasiclassical electrostatic attraction (ΔE_{elstat}) and quantum chemical σ and π interactions ($\Delta E_{orb}+\Delta E_{Pauli}$) according to energy decomposition analysis.

Molecule	Bond type	Molecule	Bond type
Li_2	$\sigma+\Delta E_{elstat}$	Na_2	$\sigma+\Delta E_{elstat}$
Be_2	ΔE_{elstat}	Mg_2	ΔE_{elstat}
B_2	$\pi+\Delta E_{elstat}$	Al_2	$\pi+\Delta E_{elstat}$
C_2	π	Si_2	ΔE_{elstat}
N_2	ΔE_{elstat}	P_2	ΔE_{elstat}
O_2	ΔE_{elstat}	S_2	ΔE_{elstat}
F_2	$\sigma+\Delta E_{elstat}$	Cl_2	$\sigma+\Delta E_{elstat}$

weaker bond in F_2 compared with Cl_2 comes from weaker quasiclassical electrostatic attraction. Another recently reported example concerns the trend of the bond strength in phosphane complexes $[W(CO)_5(PX_3)]$ (X = Me, F, Cl). The complexes $[W(CO)_5(PCl_3)]$ and $[W(CO)_5(PF_3)]$ have weaker metal–phosphane bonds than $[W(CO)_5(PMe_3)]$, although the first two species have bigger ΔE_{orb} and smaller ΔE_{Pauli} values.[34] The stronger bond in the last-named complex comes from the much larger ΔE_{elstat} value, which compensates for weaker orbital attraction and larger Pauli repulsion.

Conclusion

The equilibrium geometry of a covalent bond between elements of the second and higher rows of the periodic table is not determined by the maximum overlap of the σ valence orbitals, which nearly always has its largest value at a distance that is clearly shorter than the equilibrium bond length. The crucial interaction which prevents shorter bonds is not the loss of attractive interaction, but the sharp increase in the Pauli repulsion between electrons in valence orbitals. The attractive (ΔE_{orb}) and repulsive interactions (ΔE_{Pauli}) are both determined by the orbital overlap. The net effect of the two terms depends on the occupation of the valence orbitals, but the onset of attractive orbital interactions occurs at longer distances than Pauli repulsion, because the overlap of occupied orbitals with vacant orbitals starts earlier than overlap between occupied orbitals.

An important factor that is usually not considered for covalent bonds is the quasiclassical electrostatic interaction. The contribution of ΔE_{elstat} in most nonpolar covalent bonds is strongly attractive. This comes from the deviation of the quasiclassical electron–electron repulsion and nuclear–electron attraction from the values predicted by Coulomb's law for point charges. The actual strength of ΔE_{elstat} depends on the size and the shape of the occupied valence orbitals. The attractive electrostatic contributions in the diatomic molecules Li_2–F_2 come from the s and p(σ) electrons, while the p(π) electrons do not compensate for nuclear–nuclear repulsion. It is the interplay of the three terms ΔE_{orb}, ΔE_{Pauli}, and ΔE_{elstat} that determines the bond energies and equilibrium distances of covalently bonded molecules. Molecules like N_2 and O_2, which are usually considered as covalently bonded, would not be bonded without the quasiclassical attraction which comes from the ΔE_{elstat} term.

Acknowledgements

This paper was written while one of us (G.F.) spent a sabbatical at the Vrije Universiteit Amsterdam. He expresses his gratitude to Prof. E. J. Baerends and his group for their hospitality and support. This work was supported by the Deutsche Forschungsgemeinschaft and by the Netherlands organization for Scientific research (NWO-CW). Excellent service by the HRZ Marburg is gratefully acknowledged.

[1] R. J. Gillespie, P. L. A. Popelier, *Chemical Bonding and Molecular Geometry. From Lewis to Electron Densities*, Oxford University Press, New York, **2001**.
[2] a) G. Frenking, *Angew. Chem.* **2003**, *115*, 152; *Angew. Chem. Int. Ed.* **2003**, *42*, 143; b) R. J. Gillespie, *Angew. Chem.* **2003**, *115*, 3452; *Angew. Chem. Int. Ed.* **2003**, *42*, 3331; c) G. Frenking, *Angew. Chem.* **2003**, *115*, 3456; *Angew. Chem. Int. Ed.* **2003**, *42*, 3335.
[3] a) M. Lein, G. Frenking in *Theory and Applications of Computational Chemistry: The First 40 Years* (Eds.: C. E. Dykstra, G. Frenking, K. S. Kim, G. E. Scuseria), Elsevier, Amsterdam, **2005**, p. 367; b) G. Frenking, K. Wichmann, N. Fröhlich, C. Loschen, M. Lein, J. Frunzke, V. M. Rayón, *Coord. Chem. Rev.* **2003**, *238–239*, 55; c) A. Kovács, C. Esterhuysen, G. Frenking, *Chem. Eur. J.* **2005**, *11*, 1813; d) C. Esterhuysen, G. Frenking, *Theor. Chem. Acc.* **2004**, *111*, 381;
[4] a) H. Verbraak, J. N. P. van Stralen, J. Bouwman, J. de Klerk, D. Verdes, H. Linnartz, F. M. Bickelhaupt, *J. Chem. Phys.* **2005**, *123*, 144305; b) F. M. Bickelhaupt, R. L. DeKock, E. J. Baerends, *J. Am. Chem. Soc.* **2002**, *124*, 1500; c) C. Fonseca Guerra, F. M. Bickelhaupt, *Angew. Chem.* **2002**, *114*, 2194; *Angew. Chem. Int. Ed.* **2002**, *41*, 2092; d) F. M. Bickelhaupt, F. Bickelhaupt, *Chem. Eur. J.* **1999**, *5*, 162; e) F. M. Bickelhaupt, A. Diefenbach, S. V. de Visser, L. J. de Koning, N. M. M. Nibbering, *J. Phys. Chem. A* **1998**, *102*, 9549; f) F. M. Bickelhaupt, T. Ziegler, P. von R. Schleyer, *Organometallics* **1996**, *15*, 1477.
[5] The presence of occupied π and δ orbitals in a molecule is not synonymous with multiple bonding. By definition, a π orbital is antisymmetric with respect to a mirror plane while a δ orbital is antisymmetric with respect to two mirror planes. According to this definition, a saturated molecule which has a mirror plane always has π orbitals but it does not have a double bond.
[6] a) E. Hückel, *Z. Phys.* **1930**, *60*, 423; b) E. Hückel, *Z. Elektrochem. Angew. Phys. Chem.* **1930**, *36*, 641.
[7] E. Hückel, *Z. Phys.* **1931**, *70*, 204.
[8] J. E. Lennard-Jones, *Trans. Faraday Soc.* **1929**, *25*, 668.
[9] L. Pauling, *J. Am. Chem. Soc.* **1931**, *53*, 1367.
[10] W. Heitler, F. London, *Z. Phys.* **1927**, *44*, 455.
[11] a) K. P. Huber, G. Herzberg, *Molecular Spectra and Molecular Structure IV. Constants of Diatomic Molecules*, Van Nostrand-Reinhold, New York, **1979**; b) M. Dupuis, B. Liu, J. *Chem. Phys.* **1978**, *68*, 2902.
[12] M. Hachey, S. P. Karna, F. Grein, *J. Phys. B* **1992**, *25*, 1119.
[13] a) M. A. Spackman, E. N. Maslen, *J. Phys. Chem.* **1986**, *90*, 2020; b) F. L. Hirshfeld, S. Rzotkiewicz, *Mol. Phys.* **1974**, *27*, 1319.
[14] For a thorough discussion of the physical mechanism of the chemical bond, see references [24a, 25].
[15] For recent controversies about the role of chemical bonding models, see a) R. F. W. Bader, *Chem. Eur. J.* **2006**, *12*, 2896; b) J. Poater, M. Sola, F. M. Bickelhaupt, *Chem. Eur. J.* **2006**, *12*, 2902; c) G. Frenking, A. Krapp, S. Nagase, N. Takagi, A. Sekiguchi, *ChemPhysChem*, **2006**, *7*, 799; d) C. A. Pignedoli, A. Curioni, W. Andreoni, *ChemPhysChem*, **2006**, *7*, 801.
[16] A. D. Becke, *Phys. Rev. A* **1988**, *38*, 3098.
[17] J. P. Perdew, *Phys. Rev. B* **1986**, *33*, 8822.
[18] J. G. Snijders, E. J. Baerends, P. Vernooijs, *At. Data Nucl. Data Tables* **1982**, *26*, 483.
[19] J. Krijn, E. J. Baerends, *Fit Functions in the HFS-Method*, Internal Report (in Dutch), Vrije Universiteit Amsterdam, The Netherlands, **1984**.
[20] a) F. M. Bickelhaupt, E. J. Baerends, *Rev. Comput. Chem.* **2000**, *15*, 1; b) G. te Velde, F. M. Bickelhaupt, E. J. Baerends, S. J. A. van Gisbergen, C. Fonseca Guerra, J. G. Snijders, T. Ziegler, *J. Comput. Chem.* **2001**, *22*, 931.
[21] K. Morokuma, *J. Chem. Phys.* **1971**, *55*, 1236.
[22] a) T. Ziegler, A. Rauk, *Inorg. Chem.* **1979**, *18*, 1558; b) T. Ziegler, A. Rauk, *Inorg. Chem.* **1979**, *18*, 1755.
[23] F. M. Bickelhaupt, N. M. M. Nibbering, E. M. van Wezenbeek, E. J. Baerends, *J. Phys. Chem.* **1992**, *96*, 4864.

[24] The term "quasiclassical" was suggested by Ruedenberg: K. Ruedenberg, *Rev. Mod. Phys.* **1962**, *34*, 326. One referee pointed out that "quasiclassical" has also been used in valence bond theory for another type of interaction which includes Pauli repulsion: a) J. M. Galbraith, E. Blank, S. Shaik, P. C. Hiberty, *Chem. Eur. J.* **2000**, *6*, 2425; b) S. Shaik, A. Shurki, D. Danovich, P. C. Hiberty, *Chem. Rev.* **2001**, *101*, 1501; c) S. Shaik, P. C. Hiberty, *Rev. Comp. Chem.* **2004**, *20*, 1.

[25] W. Kutzelnigg in *The Concept of the Chemical Bond, Vol. 1* (Ed.: Z. B. Maksic), Springer Berlin/Heidelberg, **1990**, p. 1.

[26] Note that in the paper by Spackman and Maslen[13] the atoms were calculated with a spherically symmetrical electron density. This yields different values for the quasiclassical electrostatic interaction for atoms which have nonisotropic charge distributions. It has been shown that for the analysis of the actual electron density in a diatomic molecule one should better arrange the atoms such that their spatial orientation agrees with bond formation: W. H. E. Schwarz, L. Mensching, K. Ruedenberg, P. Valtazanos, L. L. Miller, R. Jacobson, W. von Niessen, *Angew. Chem.* **1989**, *101*, 605; *Angew. Chem. Int. Ed. Engl.* **1989**, *28*, 597.

[27] For a further explanation, see G. Herzberg, *Molecular Spectra and Molecular Structure. I. Spectra of Diatomic Molecules*, reprint of 2nd ed., Krieger Publishing, Malabar, FL, **1989**, p. 25, 318.

[28] The ΔE_{Pauli} curve converges toward a value of about -3 kcal mol^{-1}. The contribution of the SIE to the ΔE_{Pauli} values of the heavier elements E_2 appears to be smaller. This becomes evident from Figures 6–10, which do not exhibit negative ΔE_{Pauli} values.

[29] The ΔE_{elstat}(e–e)/e_l value gives the e–e repulsion for two electrons, while the for ΔE_{elstat}(N–e)/$e_n N_m$ value gives the N–e attraction for one electron.

[30] It may be argued that the second σ bond in Be_2 is antibonding and therefore electronic charge is removed from the interatomic region when the wavefunction becomes antisymmetrized. This should weaken the electrostatic attraction. However, the removal of electronic charge from the interatomic region of the σ* orbital is compensated by the accumulation of electronic charge of the σ orbital when hybridization with the p(σ) orbital occurs in the final step of the EDA.

[31] W. Kutzelnigg, *Angew. Chem.* **1984**, *96*, 262; *Angew. Chem. Int. Ed. Engl.* **1984**, *23*, 272.

[32] The $^1\Sigma_g^+$ state of Si_2 with the valence configuration $(2\sigma_g)^2(2\sigma_u)^2(1\pi)^4$ is even higher lying than the $^1\Sigma_g^+$ state with the valence configuration $(2\sigma_g)^2(2\sigma_u)^2(3\sigma_g)^2(1\pi)^2$: a) C. C. Arnold, T. N. Kitsopoulos, D. M. Neumark, *J. Chem. Phys.* **1993**, *99*, 766; b) T. N. Kitsopoulos, C. J. Chick, Y. Zhao, D. M. Neumark, *J. Chem. Phys.* **1991**, *95*, 1441.

[33] a) K. Fukui, *Theory of Orientation and Stereoselection*, Springer, Berlin, **1975**; b) R. B. Woodward, R. Hoffmann, *The Conservation of Orbital Symmetry*, Verlag Chemie, Weinheim, **1970**; c) T. A. Albright, J. K. Burdett, M. H. Whangbo, *Orbital Interactions in Chemistry*, Wiley, New York, **1985**; d) A. Diefenbach, F. M. Bickelhaupt, G. Frenking, *J. Am. Chem. Soc.* **2000**, *122*, 6449.

[34] G. Frenking, K. Wichmann, N. Fröhlich, J. Grobe, W. Golla, D. Le Van, B. Krebs, M. Läge, *Organometallics* **2002**, *21*, 2921.

Received: April 21, 2006
Published online: October 6, 2006

